SECTION III

PUBLISHED PAPERS
IN
JOURNALS
AND
CONFERENCE PROCEEDINGS

(JULY 1979-JUNE 1980)

Observation of Isoscalar Giant-Resonance Structure in the Fission of ^{238}U Following Inelastic Scattering of ^{6}Li

A. C. Shotter
Physics Department, University of Edinburgh, Edingurgh EH9 3JZ, United Kingdom, and Lawrence Berkeley Laboratory, Berkeley, California 94720

and

C. K. Gelbke and T. C. Awes
Physics Department, Michigan State University, East Lansing, Michigan 48824, and Lawrence Berkeley Laboratory, Berkeley, California 94720

and

B. B. Back
Chemistry Division, Argonne National Laboratory, Argonne, Illinois 60439

and

J. Mahoney, T. J. M. Symons, and D. K. Scott
Lawrence Berkeley Laboratory, Berkeley, California 94720
(Received 8 June 1979)

Resonance structures are observed in the region of the isoscalar giant quadrupole resonance for the reaction $^{238}U(^{6}Li, ^{6}Li'f)$ at 150 MeV. The ratio between the fission probabilities of resonance and compound-nucleus components appears to be greater than the recently reported value from (α,α') scattering.

Several experiments have been undertaken to investigate the decay modes of the isoscalar giant quadrupole resonance in the actinide nuclei. Electron scattering and photoabsorption have provided indirect evidence that the fission probability for the quadrupole resonance is greater than that for the dipole resonance.[1] A recent study[2] of the $(\alpha,\alpha'f)$ reaction on ^{232}Th and ^{238}U targets arrived at the conclusion that the fission decay of the giant quadrupole resonance is inhibited by at least a factor of 5 as compared with the fission decay of the continuum, since no resonance structure was observed in this channel. We report here the measurement of the fission decay of ^{238}U induced by the inelastic scattering of ^{6}Li where clear resonance structure is observed in the fission channel.

Self-supporting metallic ^{238}U targets of 0.5-mg/cm^2 thickness were bombarded with 150-MeV $^{6}Li^{3+}$ ions from the 88-in. cyclotron of the Lawrence Berkeley Laboratory. The experiment was performed in two parts. First, singles spectra of inelastically scattered ^{6}Li nuclei were measured with a magnetic spectrograph; this avoids the background problems due to nuclear reactions in solid-state detectors. Second, inelastic ^{6}Li spectra corresponding to coincidences between ^{6}Li nuclei and fission fragments were measured with the experimental arrangement shown in Fig. 1. The fission fragments were detected with large-area parallel-plate proportional detectors *A* and *B* and the ^{6}Li nuclei were detected with a solid-state telescope placed either in (I) or out (O) of the horizontal plane. Solid-state detectors could be used for this part of the experiment since the coincidence requirement considerably reduces the background.

An example of a singles ^{6}Li spectrum taken at 16° with the magnetic spectrograph is shown in Fig. 2; the contributions from carbon and oxygen were measured in separate experiments and have been subtracted in Fig. 2. It was discovered that the shape of the energy spectrum did not change

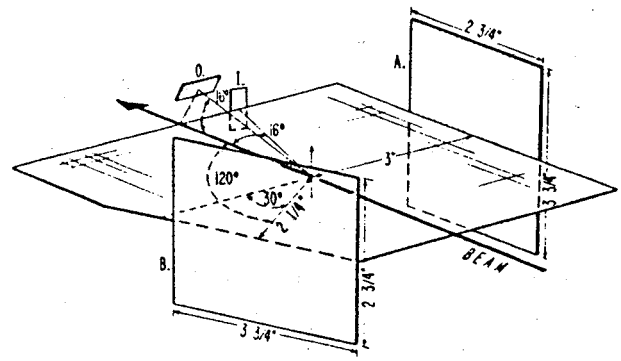

FIG. 1. Experimental layout for the coincidence experiment.

Low-Energy Pion Production at 0° with Heavy Ions from 125 to 400 MeV/Nucleon

W. Benenson, G. Bertsch, G. M. Crawley, E. Kashy, and J. A. Nolen, Jr.
Cyclotron Laboratory and Physics Department, Michigan State University, East Lansing, Michigan 48824

and

H. Bowman, J. G. Ingersoll, J. O. Rasmussen, and J. Sullivan
Lawrence Berkeley Laboratory, University of California, Berkeley, California 94720

and

M. Koike
Institute of Nuclear Science, Tokyo, Japan, and Lawrence Berkeley Laboratory, Berkeley, California 94720

and

M. Sasao
Physics Department, Osaka University, Osaka, Japan, and Lawrence Berkeley Laboratory, Berkeley, California 94720
and

J. Péter
Institut de Physique Nucléaire, Orsay, France

and

T. E. Ward
Indiana University Cyclotron Facility, Bloomington, Indiana 47401
(Received 30 April 1979)

The results of a systematic study of 0° pion production by heavy ions from 125 to 400 MeV/nucleon are presented. The dependence of the cross section on the mass number of the target, the energy of the beam, and the pion charge and energy are discussed. A striking feature of the data is an unexpectedly large π^-/π^+ ratio for pions of velocity close to the projectile velocity.

There has been much speculation in recent years on the possibilities of a variety of qualitatively new nuclear phenomena[1-4] which may be observable with the pions produced in heavy-ion collisions. Detailed studies of pion production in such collisions with beam energies below ~1 GeV/nucleon are currently being carried out by several groups[5-8] to quantify the pion-production reaction mechanism and possibly to discover one of these new phenomena. In this Letter we present the first results from an experiment designed for pion measurements in a kinematic regime not previously investigated in heavy-ion experiments, namely, pions emitted at 0° with near-zero kinetic energy in the center-of-mass and projectile frames.

The 180° magnetic spectrometer used in this work has permitted measurements of both π^+ and π^- emitted with kinetic energy between 34 and 155 MeV in the laboratory system. At 400 MeV/nucleon this includes pions emitted with energies well below the Coulomb barrier in the center-of-mass and projectile frame. An unexpected result of these measurements is the very sharp and large anomaly in the π^-/π^+ cross-section ratio R displayed in Fig. 1. Additional results made possible by this apparatus include quantitative measurements of pion-production cross sections at heavy-ion-beam energies much lower than previously possible, far below the threshold for pion production in free nucleon-nucleon collisions and even below the threshold for nucleon-nucleus collisions. Spectra of π^+ and π^- have been recorded at 0° for Ne + NaF at five beam energies from 125 to 400 MeV/nucleon. Some data were also taken on Cu and U targets and at angles out to 30°.

The differential cross section at 0° varies by about four orders of magnitude over the beam energy range studied, and at the lowest energy, 125 MeV/nucleon, the pion yeild corresponds to less than one pion per 1000 nuclear interactions. The data are summarized in Fig. 2 and will be discussed further below. Preliminary theoretical considerations, also given below, indicate that a single production mechanism cannot account for the large variation of cross section over this range of beam energies.

Evidence for Orbital Dispersion in the Fragmentation of ^{16}O at 90 and 120 MeV/Nucleon

K. Van Bibber, D. L. Hendrie, D. K. Scott, H. H. Weiman,
L. S. Schroeder, J. V. Geaga, S. A. Cessin, R. Treuhaft,
Y. J. Grossiord,[a] and J. O. Rasmussen
Lawrence Berkeley Laboratory, University of California, Berkeley, California 94720

and

C. Y. Wong
Oak Ridge National Laboratory, Oak Ridge, Tennessee 37830

(Received 10 April 1979)

The parallel- and transverse-momentum distributions have been measured for fragments of $Z \geq 3$ produced by the fragmentation of ^{16}O at 90 and 120 MeV/nucleon. A strong anisotropy is observed with $\sigma_{p\perp} \approx 200$ MeV/c for all fragments, which can be explained by considering the dispersion due to orbital deflection of the projectile prior to breakup.

The understanding of the reaction mechanism in projectile fragmentation has been long sought for. At relativistic energies with ^{12}C and ^{16}O projectiles, both the abrasion-ablation calculations and models of projectile excitation followed by statistical decay adequately describe the isotope distributions.[1,2] Further, it has been pointed out that there is an exact formal degeneracy between such models with regard to the fragment momentum distributions.[3] Recent data for a

Production of Neutron-Rich Nuclides by Fragmentation of 212-MeV/amu ^{48}Ca

G. D. Westfall, T. J. M. Symons, D. E. Greiner, H. H. Heckman, P. J. Lindstrom, J. Mahoney, A. C. Shotter,[a] and D. K. Scott
Nuclear Science Division, Lawrence Berkeley Laboratory, University of California, Berkeley, California 94720

and

H. J. Crawford and C. McParland
Space Sciences Laboratory, University of California, Berkeley, California 94720

and

T. C. Awes and C. K. Gelbke
Heavy Ion Laboratory, Michigan State University, East Lansing, Michigan 48824

and

J. M. Kidd
U. S. Naval Research Laboratory, Washington, D. C. 20375
(Received 15 October 1979)

Yields of neutron-rich projectile fragments have been measured at 0° for the reaction of 212-MeV/amu ^{48}Ca ions on an 890-mg-cm^{-2} beryllium target. Fourteen nuclides have been observed for the first time. The systematics of production cross sections are discussed.

The limits of stability for nuclei have been established up to sodium and beryllium for proton-rich and neutron-rich nuclides, respectively. Recently, the techniques of relativistic heavy-ion fragmentation,[1] deeply inelastic scattering,[2] and spallation induced by high-energy protons[3] have been used to produce neutron-rich nuclei near the limit of particle stability. In this Letter, we present the first experimental evidence for the particle stability of fourteen nuclides, ^{22}N, ^{26}F, ^{33,34}Mg, ^{36,37}Al, ^{38,39}Si, ^{41,42}P, ^{43,44}S, and ^{44,45}Cl, produced in the fragmentation of 212-MeV/amu ^{48}Ca. In addition, the recent observation[2] of ^{37}Si, ^{40}P, and ^{41,42}S is confirmed. Predictions for the masses of neutron-rich light nuclei have been made based on several methods, including iterative techniques such as the modified Garvey-Kelson relations,[4,5] the liquid-droplet model,[6,7] and large-basis shell-model calculations.[8] The energy levels of such nuclei have also been predicted using the same shell-model calculations.[8,9] From the present experiment it appears that the production cross sections for very neutron-rich light nuclei may be quite sensitive to their detailed nuclear structure.

The experimental arrangement used for the present work was similar to that described in Ref. 1. The fragments, which emerge from the reaction at nearly the beam velocity, were detected in a zero-degree magnetic spectrometer with an acceptance of 0.94 msr. A detector telescope consisting of twelve Si(Li) detectors, two position-sensitive Si(Li) detectors (PSD), and a veto scintillator was placed in the focal plane of the spectrometer. Each of the twelve Si(Li) detectors was 5 mm thick and 5 cm in diameter while the PSD's were 500 μm thick and 6 cm in diameter. The PSD's were arranged to measure horizontal and vertical position with a resolution of ~1 mm. The beam current of ^{48}Ca ions from the Bevalac was ~10^7 particles/sec and was monitored directly with plastic scintillators, an ion chamber, and a scintillator telescope that monitored particles scattered from the target. The target consisted of 890 mg cm^{-2} of beryllium and the beam lost approximately 35 MeV/amu passing through it.

Combining the spectrometry with the energy-loss measurements in the Si(Li) detectors made it possible to measure M and Z unambiguously as described in Ref. 1. The mass resolution obtained was 0.3 amu. The mass- and atomic-number scales were calibrated by use of the direct ^{48}Ca beam and also beams of ^{20}Ne and ^{40}Ar of high energy that were progressively degraded to provide a continuous spectrum of ^{20}Ne and ^{40}Ar ions stopping in each detector. Since the detector thicknesses were precisely known, it was then possible to use a range-energy table to make an accurate channel-to-energy calibration for each detector assuming accurate extrapolations to the measured neutron-rich nuclei.

Effective Interaction for Charge-Exchange Analogs of Gamow-Teller Transitions

Sam M. Austin, L. E. Young,[a] R. R. Doering,[b] R. DeVito, R. K. Bhowmik,[c] and S. D. Schery[d]
Cyclotron Laboratory and Physics Department, Michigan State University, East Lansing, Michigan 48824

(Received 14 January 1980)

Ratios of cross sections for ^{7}Li$(p,n)^7$Be leading to the ground and first excited states of ^{7}Be have been measured at 24.8, 35, and 45 MeV. An analysis of these ratios yields the ratio of spin-flip to spin-nonflip strength, $|V_{\sigma\tau}/V_\tau|^2$, free of many of the uncertainties usually associated with distorted wave analyses for such light nuclei. The ratio increases by about 60% in the observed energy range. A comparison with known values of V_τ yields $V_{\sigma\tau}$. The isovector tensor force is also obtained.

It has been recognized for some time that the operators mediating charge exchange via hadronic reactions and β decay are identical in spin-isospin space, so that strong transitions observed in a (p,n) reaction should also be strong in β decay.[1] Charge exchange without spin transfer (mediated by the two-body effective interaction $V_\tau \vec{\tau}_1 \cdot \vec{\tau}_2$) corresponds to Fermi β decay and with spin flip [mediated by $V_{\sigma\tau}(\vec{\sigma}_1 \cdot \vec{\sigma}_2)(\vec{\tau}_1 \cdot \vec{\tau}_2)$] to Gamow-Teller β decay. Recently this correspondence has been exploited to search with (p,n) and $(^3\mathrm{He},t)$ reactions for Gamow-Teller strength in nuclei.[2] There are strong indications[2] that such strength is concentrated in 1^+ states located near the isobaric analog state in $^{90-96}$Nb and $^{112-124}$Sb. However, quantitative evaluation of the observed strength can only be made when one has a reliable estimate of $V_{\sigma\tau}$. Unfortunately only a little empirical information is available[3] and since that is for light nuclides (mostly $A=6$ and 7) the results are subject to substantial model uncertainties. Theoretical estimates have been made[4] but those for $V_{\sigma\tau}$ have not been tested against experiment to any great extent.

In this Letter we present the results of a measurement, at 25, 35, and 45 MeV, of the *ratio* of the cross sections σ_0 and σ_1, for the reaction ^{7}Li$(p,n)^7$Be leading to the ground $(\frac{3}{2}^-)$ and first excited $(\frac{1}{2}^-$, 0.429 MeV) states of ^{7}Be (see Fig. 1). Anderson, Wong, and Madsen[5] (AWM) noted some time ago that σ_1 and σ_0 depend differently on $V_{\sigma\tau}$ and V_τ and that cross-section ratios could be analyzed in a simple model, discussed later, to yield $V_{\sigma\tau}/V_\tau$ with most of the model dependence vanishing in the ratio. However, until now, limitations on energy resolution for neutrons have made it impossible to separate the yields of the two states at energies above 25 MeV. An analysis of our measured ratios with the simple model of AWM indicates that $|V_{\sigma\tau}/V_\tau|^2$ increases by about 60% between 25 and 45 MeV. Should this increase continue, spin-flip transitions will dominate the spin-nonflip ones above about 65 MeV and studies at these energies will be extremely useful in searches for concentrations of spin-flip strength in nuclei. A detailed distorted-wave Born-approximation (DWBA) analysis carried out at $E_p = 35$ MeV indicates that the approximations of AWM are realistic and yields as a by product a more reliable estimate of the tensor force than has been available in this energy range. Values of $V_{\sigma\tau}$ were obtained from $V_{\sigma\tau}/V_\tau$ and known values of V_τ.[3]

The measurements were performed with protons from the Michigan State University sector-focused cyclotron and a time-of-flight system[6]

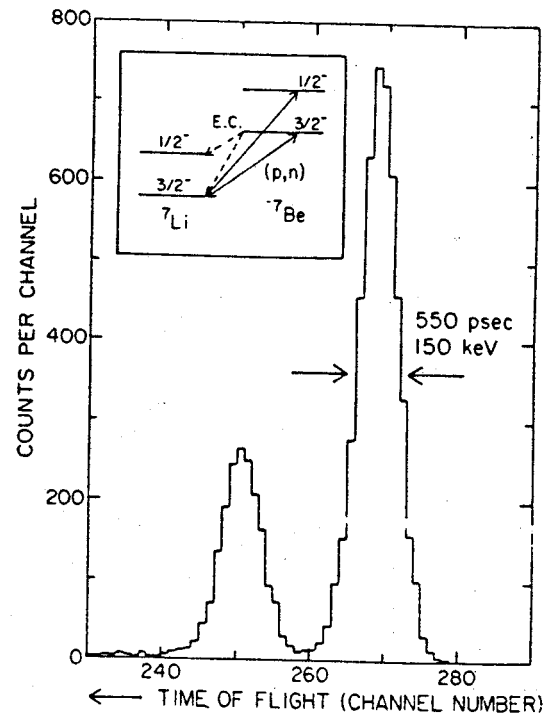

FIG. 1. Neutron time-of-flight spectrum from the reaction ^{7}Li$(p,n)^7$Be. Time of flight increases to the left. The overall time resolution is 550 psec corresponding to an energy resolution of $\simeq$ 150 keV. The inset shows the (p,n) transitions involved and the electron-capture transitions involved in the analysis.

ENERGY DEPENDENCE OF MULTINUCLEON TRANSFER REACTIONS INDUCED BY ^{20}Ne ON ^{12}C

M.E. ORTIZ, A. DACAL and A. MENCHACA-ROCHA
Instituto de Fisica, UNAM, México 20, D.F., Mexico

and

M. BUENERD [1], D.L. HENDRIE [2], J. MAHONEY, C. OLMER [3] and D.K. SCOTT
Lawrence Berkeley Laboratory, Berkeley, CA 94720, USA

Received 13 February 1979

The energy dependence of up to five nucleon transfer reactions induced by ^{20}Ne on ^{12}C has been measured in the energy range 150 to 294 MeV. Good agreement is found between the experiment and both DWBA and semiclassical calculations.

Systematic studies of multi-nucleon transfer reactions induced by heavy ions, involving both variations in incident energy and mass transfer can make a stringent test of heavy-ion reaction mechanisms. We have investigated the energy dependence of multi-nucleon transfer reactions on a light target nucleus through the measurement of reactions of the type ^{12}C(^{20}Ne, x)Y, where x ranges from ^{19}F to ^{15}N (i.e. from one to five nucleon transfers) at incident energies of 150, 175, 202, 225, 252 and 294 MeV. In this letter we show that the gross features of the incident energy and mass transfer dependences of the reactions can be well reproduced by either DWBA or semiclassical calculations.

The ^{20}Ne$^{5+,6+}$ beams from the 88-Inch Berkeley Cyclotron were used to bombard solid ^{12}C targets of thickness 100 μg/cm^2. The reaction products were detected and identified using a QSD spectrometer and a focal plane detector [1]. The overall energy resolution of 150 keV (fwhm) was mainly determined by kinematics and target thickness.

The energy spectra measured for the reaction product ^{16}O at forward angles are shown in fig. 1 at several incident energies. The other reaction products (^{19}F,

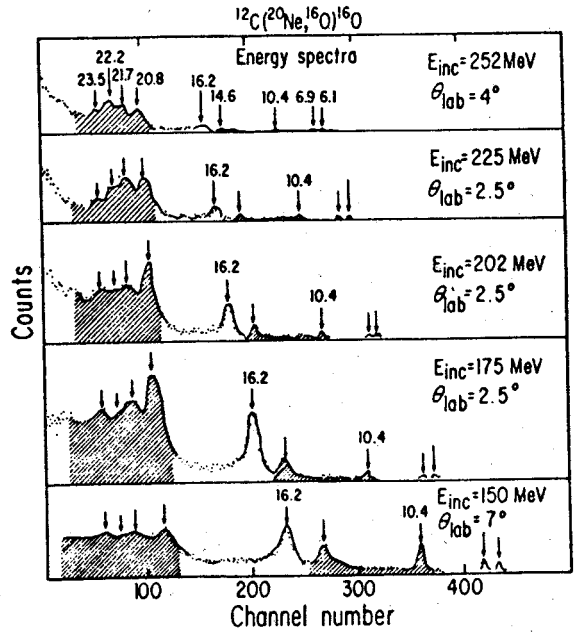

Fig. 1. The energy spectra for the reaction ^{12}C(^{20}Ne,^{16}O)^{16}O measured at forward angles are shown as a function of incident energy. The shaded region represents the excitation energy windows considered for the analysis of the energy dependence.

[1] Permanent address: Institut des Sciences Nucléaires, Cedex 257, 38044 Grenoble, France.
[2] Present address: Department of Physics and Astronomy, University of Maryland, College Park, MD 20742, USA.
[3] Present address: Physics Division, Argonne National Laboratory, Argonne IL 60439, USA.

NEGATIVE-PARITY YRAST BAND IN ^{170}Yb: ROTATION-ALIGNED NEUTRONS WITH DEFORMATION-COUPLED BANDHEAD?

P.M. WALKER, S.R. FABER, W.H. BENTLEY, R.M. RONNINGEN, R.B. FIRESTONE and F.M. BERNTHAL

Departments of Physics and Chemistry and Cyclotron Laboratory, Michigan State University, East Lansing, MI 48824, USA

Received 9 July 1979

A sideband in ^{170}Yb has been identified up to $I^{\pi} = 17^{-}$. It has an isomeric $I = 4$ bandhead, yet the odd-spin states have prompt branches to the ground-state band. The contrasting properties are explained by the Coriolis effects on the quasiparticle configuration.

Low-lying negative-parity sidebands are now a well-established feature of deformed even–even nuclei. The lowest such sideband is conveniently termed the negative-parity yrast band. In the prolate rare-earth region these sidebands usually have some considerable fraction of the intrinsic angular momentum aligned with the collective rotation [1] by the Coriolis interaction. This yields high apparent moments of inertia, though the systematics extend to the low moment-of-inertia octupole bands in the heavier part of the deformed region (with $N \gtrsim 102$). The theoretical interpretation in terms of quasiparticles coupled to a rotating core [2] makes clear the importance of the high-j, $i_{13/2}$ neutrons. However, γ-ray spectroscopic evidence to support the $i_{13/2}$ assignment has not been available. This is at least partly a consequence of the decoupled structure of the bands, making the unfavored even-spin members hard to observe in (i, xn) reactions, and even when they are identified [3–6], the in-band $J \rightarrow J - 1$ transitions are too weak (or poorly resolved) to allow useful spectroscopic evidence to be gained.

The present paper reports on the observation to high spin of a negative-parity yrast band where the in-band $J \rightarrow J - 1$ transitions are used to identify the dominant particle configuration. The unusual features of this band are explained as a consequence of its quasiparticle structure.

Levels in ^{170}Yb have been populated following the ^{168}Er(α, 2n)^{170}Yb and ^{170}Er(α, 4n)^{170}Yb reactions, at 27 MeV and 50 MeV, respectively, with α-particle beams provided by the MSU cyclotron. Singles and coincidence γ-ray and conversion-electron measurements were made to characterise the observed radiations. The backbending in the positive-parity yrast band reported by Hartley et al. [7] is confirmed, and the $20^{+} \rightarrow 18^{+}$ transition is tentatively assigned at 630.8 keV. Several sidebands have been identified [8] in the present work, including the negative-parity yrast band. The levels of this band, along with those in the positive-parity yrast band, are illustrated in fig. 1. The basic scheme is established by γ-ray coincidences, and the spin assignments are made on the basis of six-point angular distributions. The negative parity of the sideband is established from the small electron conversion coefficients for the 908.7 and 999.5 keV transitions, both of which have $\alpha_K < 3 \times 10^{-3}$. This result permits either E2 or E1 assignments, but the angular distributions establish almost pure dipole character, and hence the negative parity.

The 350 ns half-life of the 1258.7 keV, 4^{-} level is obtained from the time spectrum for the 981.1 keV transition. This yields a Weisskopf hindrance factor of 1.5×10^{9} for the transition (assuming E1 multipolarity) which compares well with the other known values [9] for E1, $\Delta K = 4$ transitions. Considering that the decay is to the $K = 0$ ground-state band (gsb) it is reasonable to assign a value of $K = 4$ to the $I = 4$,

THE EFFECT OF THE N* (1688) RESONANCE ON NUCLEAR CHARGE FORM FACTORS ☆

D.O. RISKA
Department of Physics, Michigan State University, East Lansing, MI 48824, USA

Received 2 July 1979

Empirical information on resonant pion photoproduction amplitudes and quark model estimates for the γNN* coupling strength indicate that the pion exchange charge operator with an intermediate N*(1688) is of far less significance for nuclear charge form factors than the pair exchange current. The size of the effect depends strongly on the D-state admixtures in the wavefunctions.

It has recently been suggested by Kisslinger [1] that the pion exchange charge operator with an intermediate N*(1688) resonance, illustrated by the diagrams in fig. 1, could lead to a very large correction to the calculated charge form factor of ^{3}He. The importance of this point is emphasized by the systematic difficulties encountered in explaining the charge form factors at high-momentum transfer of nuclei throughout the periodic table with realistic wavefunctions, even when the conventional pion "pair" exchange operator is taken into account [2]. We shall here, however, show that the present empirical information on resonant pion photoproduction and quark model estimates for the resonance photocouplings indicate that in fact the pion exchange charge operator involving the N* (1688) is actually far less important for nuclear charge form factors than the much investigated "pair" operator obtained from the nonrelativistic limit of the nucleon pole term in the photoproduction amplitude. The relative magnitude of the N* (1688) effect turns out to be very sensitive to the amount of D-state admixture in the ground state wavefunctions of the light nuclei.

In order to construct the two-body charge operator associated with the Feynman diagrams in fig. 1 we use the phenomenological πNN* and γNN* lagrangians [3]:

☆ Research supported in part by the National Science Foundation.

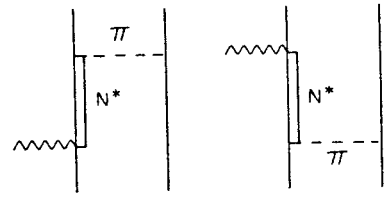

Fig. 1. The diagrams describing the pion exchange charge operator involving the N*(1688) resonance.

$$\mathcal{L}_{\pi NN^*} = i\frac{f^*}{m_\pi^2}\bar{\psi}\partial_\mu\partial_\nu\boldsymbol{\phi}\cdot\boldsymbol{\tau}\gamma_5\psi_{\mu\nu} + \text{h.c.}, \quad (1)$$

$$\mathcal{L}_{\gamma NN^*} = ie\frac{g^*}{m_\pi}\bar{\psi}\left[\partial_\nu A_\mu - \frac{1}{m^* - m}\partial_\mu\partial_\nu(\gamma A)\right]\psi_{\mu\nu} + \text{h.c.} \quad (2)$$

Here ψ and $\boldsymbol{\phi}$ are the nucleon and pion field operators, A_μ the electromagnetic field and $\psi_{\mu\nu}$ the double vector -spinor describing the spin 5/2 particle. The masses of the pion, nucleon and N* are denoted m_π, m and m^*, respectively.

The magntiude of the πNN* coupling constant f^* can be determined from the relevant partial width of the N* (0.6 × 140 MeV) to be $f^{*2}/4\pi \approx 0.014$. In order to determine the sign of f^* one must resort to a quark model. Using the harmonic oscillator quark model [4] to describe the nucleon ($L = 0^+$, $\underline{56}$) and the N* ($L = 2^+$, $\underline{56}$) one obtains

LIGHT-PARTICLE SPECTRA OBSERVED IN CENTRAL AND PERIPHERAL COLLISIONS OF $^{16}O + ^{238}U$ AT 20 MeV/NUCLEON

T.C. AWES and C.K. GELBKE
Heavy Ion Laboratory, Michigan State University, East Lansing, MI 48824, USA
and Lawrence Berkeley Laboratory, University of California, Berkeley, CA 94720, USA

B.B. BACK, A.C. MIGNEREY and K.L. WOLF
Chemistry Division, Argonne National Laboratory, Argonne, IL 60439, USA

P. DYER
Heavy Ion Laboratory, Michigan State University, East Lansing, MI 48824, USA

and

H. BREUER and V.E. VIOLA Jr.
Department of Chemistry, University of Maryland, College Park, MD 20742, USA

Received 29 June 1979

Energetic light particles have been measured in coincidence with two outgoing fission fragments which result from the reaction $^{16}O + ^{238}U$ at 315 MeV. Central and peripheral collisions can be distinguished by the momentum transferred to the target residue as deduced from the angle between coincident fission fragments. A remarkable similarity is observed in the forward angle light particle spectra observed in peripheral and central collisions.

The emission of energetic light particles [1] in heavy-ion reactions at non-relativistic energies has attracted renewed interest both experimentally [1–9] and theoretically [10–14]. At present, however, little is known about the relative importance of peripheral and central collisions for the production of these particles. In this letter we address ourselves to this question by measuring the angle between two coincident fission fragments [15–16] to discriminate between central and peripheral collisions.

The experiment was performed at the 88 inch cyclotron of the Lawrence Berkeley Laboratory. A $^{238}UF_4$ target of 200 $\mu g/cm^2$ thickness mounted on a 50 $\mu g/cm^2$ carbon backing was bombarded with $^{16}O^{6+}$ ions of 315 MeV energy. Light particles (p, d, t, α) were detected at 14° with a ΔE–E telescope consisting of a 350 μm thick solid state ΔE-detector and a $1\frac{1}{2}$ inch thick NaI E-detector. An aluminum absorber of 1 mm thickness was placed in front of this telescope to stop heavy particles ($Z > 3$). In addition, two solid-state detector telescopes were installed to detect alpha particles at 30° and heavy ions (Li, ... , O) at 15°. A lower threshold of 40 MeV was placed on both alpha particle spectra in the final analysis. Two fission fragments emitted in coincidence with light particles were detected by two position-sensitive solid-state detectors, each subtending the angular range of 62°–98° and mounted in a plane with the light particle telescopes. In addition to the measurements at 315 MeV a short calibration run was also performed at 140 MeV beam energy.

The momentum transferred to the target residue can be written as

$$p_R = p_A + p_B \,, \qquad (1)$$

where the indices R, A, and B denote the target residue

OBSERVATION OF PARTICLE ALIGNMENT IN THE OCTUPOLE BAND OF ^{172}Yb

P.M. WALKER, S.R. FABER, W.H. BENTLEY, R.M. RONNINGEN and R.B. FIRESTONE
Departments of Physics and Chemistry and Cyclotron Laboratory, Michigan State University, East Lansing, MI 48824, USA

Received 7 August 1979

Members of the octupole band up to spin 14^- have been identified with the ^{170}Er(α,2n)^{172}Yb reaction. The band is strongly perturbed by Coriolis effects and has a high moment of inertia with variations characteristic of particle alignment. Vibrational alignment is insufficient to explain the data.

Most of the negative-parity yrast bands in deformed even–even nuclei can be divided into two types, those appearing as aligned two-quasiparticle bands with high moments of inertia, typical of prolate nuclei with $A \approx 160$, and those bands based on the single-phonon octupole vibration with relatively low moments of inertia, typical of prolate nuclei with $A \approx 180$. The latter have been described by Neergård and Vogel [1] who show the importance of the contributing two-quasiparticle configurations, while a possible change from octupole structure to particle-aligned structure at high spin is discussed by Vogel [2]. Although irregularities indicative of particle alignment have been found in the $N = 88$ transitional nuclei [3], the negative-parity yrast bands in these isotones appear to be already well alligned even at low spins, and a smooth change from octupole spins, and a smooth change from octupole structure to particle-aligned structure is not yet evident in any single nucleus. Experimental verification of such a change would be an important contribution towards the understanding of the negative-parity yrast states.

A fertile region of investigation is around $N = 104$. since, for example, the heavier tungsten isotopes ($N > 104$) have well-established octupole structure, while the negative-parity yrast bands in the lighter tungsten isotopes ($N < 104$) have particle-aligned structure [4]. Recently, Sheline et al. [5] have shown that the properties of the octupole band [6] in ^{180}W ($N = 106$) may be explained in terms of the alignment of the vibrational angular momentum, without the necessity of particle alignment. Here we consider data [7] on ^{178}W ($N = 104$) for which particle alignment appears to be a necessary hypothesis, and new results for ^{172}Yb ($N = 102$) where the data are more definitive.

States in ^{172}Yb were populated by the ^{170}Er(α, 2n)^{172}Yb reaction, with 27 MeV α-particles from the MSU cyclotron incident on both oxide and metallic, isotopically enriched, targets with thicknesses from 1 to 5 mg cm^{-2}. Singles and coincidence γ-ray and conversion-electron measurements were performed to characterise the observed radiations. Several rotational bands were identified, as will be described in a future publication, but here we report on the extension of the octupole band to $I^\pi = 14^-$, as discussed below, and the ground-state band (gsb) to 14^+, previously studied by Mo et al. [8]. The energy levels of these two bands are illustrated in fig. 1, together with the transitions observed in the present study. Angular distributions typical of stretched-quadrupole transitions establish the spin sequences where in-band transitions are observed, except for the $(14^-) \rightarrow 12^-$ transition which is too weak to obtain a reliable distribution. The spin and parity assignments in the octupole band for $I \leqslant 3$ are known from neutron capture studies [9]. These levels are only weakly populated with the (α, n) reaction, but well-resolved γ-rays observed with the appropriate energies to be depopulating these lowest octupole states are included in fig. 1 as tentative transitions. States in the octupole band with $I = 3$–8 are well

EXPERIMENTAL RESOLUTION OF THE ^{145}Gd ϵ/β-DECAY BRANCHING RATIO ANOMALIES

R.B. FIRESTONE [1], R.C. PARDO [2] and Wm.C. McHARRIS

Department of Chemistry, Cyclotron Laboratory, and Department of Physics, Michigan State University, East Lansing, MI 48824, USA

Received 31 October 1979

Previously reported large anomalies in ^{145}Gd ϵ/β^+ decay branching ratios can be completely explained by improved experimental data. New, high-statistics decay-scheme data show conclusively that the anomalies resulted from numerous, formerly unobserved, weak transitions from levels in ^{145}Eu fed primarily by ϵ-decay. In addition, the ^{145}Gd β^+ endpoint is measured by $\beta-\gamma$ coincidence techniques to be 240 keV lower than originally reported.

In recent years measurements of several electron capture (ϵ) to β^+ decay branching ratios from ^{145}Gd were reported to be anomalous by factors as large as 40 from normal allowed β-decay theory [1,2]. Extension of β-decay theory through second order has shown that it is very difficult to explain anomalies greater than a factor of two [3,4]. It is therefore desirable to find an experimental explanation for these anomalies.

Hornshój et al. [5] (hereafter HNR) have suggested that they might be explained by two subtle experimental difficulties. First, they argued that the large decay energy (Q_ϵ) available to ^{145}Gd could lead to significant feeding to the many levels above 2.5 MeV in ^{145}Eu. These levels, although individually weakly fed, might deexcite with a large total intensity through those states which appear to have anomalous ratios. Because the feeding to such high-lying levels is largely from ϵ-decay, the failure to observe them would lead to an excess of apparent ϵ-decay to lower-lying states. This is consistent with the direction of the anomalies. Second, they argued that Q_ϵ for ^{145}Gd was tabulated to be too large [6]. This might occur because the existing β^+ endpoint data had not been corrected for the contribution from the highest-energy β^+ branch. A lower Q_ϵ would also tend to decrease the anomaly. HNR supported their argument solely on the basis of a ^{145}Gd γ-ray singles spectrum. In this spectrum they observed 250 new γ-rays above 2.5 MeV in energy, which they claimed to represent some 16% of the total decay intensity. In addition, they determined the endpoint of this γ-ray spectrum and inferred it to be the maximum decay energy. The endpoint determined in this manner was 300 keV lower than the tabulated value. Although these data supported their own general arguments, they could not be taken as a definite resolution of the anomalies. Indeed, HNR say that "the level density is so high that an exact determination of the γ-ray intensity balance is quite out of reach of current γ-spectroscopic techniques."

In this letter we present more definitive data which, we claim, put the anomalies to rest conclusively. Determining Q_ϵ by means of the γ-ray endpoint, as done by HNR, is at best a dubious technique because of the fact that any γ-ray spectrum is dominated by Compton events, which can give an endpoint as much as 240 keV too low. Also, chance clustering of γ-ray strength, as acknowledged by HNR, will tend to bias the endpoint unpredictably. To examine these problems more directly, we have observed $\beta-\gamma$ coincidences following ^{145}Gd decay. Sources of ^{145}Gd were produced by the ^{144}Sm (α, 3n) ^{145}Gd reaction using a 42 MeV α-beam from the MSU sector-focused cyclotron. Thin sources deposited by a He-jet recoil transport system [7] were placed between a pilot-B plastic scintillator β-detector

[1] Present address: Nuclear Science Division, Lawrence Berkeley Laboratory, Berkeley, CA 94720, USA.

[2] Present address: Physics Division, Argonne National Laboratory, Argonne, IL 60439, USA.

MASS OF ^{146}Gd AND ^{147}Gd AND SHELL CLOSURE AT $Z = 64$

R.C. PARDO [1], S. GALES [2], R.M. RONNINGEN and L.H. HARWOOD
Cyclotron Laboratory, Michigan State University, East Lansing, MI 48824, USA

Received 28 August 1979

The heavy ion reactions ^{144}Sm(^{12}C, ^{10}Be)^{146}Gd and ^{144}Sm(^{12}C, ^{9}Be)^{147}Gd have been used to measure the masses of ^{146}Gd and ^{147}Gd. The results show that the proton gap at $Z = 64$ for ^{146}Gd is approximately the same size as the $N = 82$ neutron gap in this nucleus.

Recent studies by Kleinheinz et al. [1] and Ogawa et al. [2] have shown that the first excited state at 1579 keV in ^{146}Gd is the $J^{\pi} = 3^{-}$ state. The first 2^{+} state is located at the relatively high excitation energy of 1971 keV. Only ^{208}Pb is known to have a similar level structure. These results, together with other direct information, indicate that the proton single particle energy gap at $Z = 64$, $N = 82$ between the $1g_{7/2}$ and $2d_{5/2}$ proton orbitals and the $1h_{11/2}$ orbital is quite large when compared to the neutron single particle energy gap at $N = 64$.

The nuclear masses needed to address the question of the magnitude of the gap at $Z = 64$, $N = 82$ are ^{145}Eu, ^{145,146,147}Gd, and ^{147}Tb. Only the masses of ^{145}Eu and ^{147}Gd have been reported in the literature [5]. Recently Firestone et al. [3] have measured the mass excess of ^{145}Gd to be -72.87 ± 0.06 MeV. In this paper, we report the values of the mass excess for ^{146}Gd and ^{147}Gd deduced from Q-value determinations in the reactions ^{144}Sm(^{12}C, ^{10}Be)^{146}Gd and ^{144}Sm(^{12}C, ^{9}Be)^{147}Gd.

The MSU sector-focused cyclotron provided 75 MeV $^{12}C^{4+}$ ions with beam current intensities ranging from 150 nA to over 1 μA on target. Typical intensities were 250 nA. Reaction products were detected in the focal plane of an Enge split-pole spectrograph by a two-wire charge-division transmission gas proportional counter. This counter was backed by a stopping scintillator which gave total energy and time-of-flight information. The resulting ΔE, E, and TOF data gave excellent identification of the $^{10}Be^{4+}$ and $^{9}Be^{4+}$ ions.

A new optical tuning technique described by Kashy et al. [4] was used in this experiment to obtain optimum resolution. This technique employs a MgO scintillator in the focal plane of the Enge split-pole spectrograph viewed by a television camera. The resulting resolution obtained in this experiment was as good as 90 keV for short runs. Due to the combined effects of ion source instabilities and target effects more typical resolutions were 100–120 keV. The targets used were approximately 100 μg/cm^2 ^{144}Sm (96.5%) evaporated onto a 20 μg/cm^2 ^{12}C foil backing. Similar thickness ^{92}Mo (98.3%) targets were used to calibrate the spectrograph.

Target thicknesses were determined by α-gauge measurements using α-particles from ^{232}Th decay products. For the estimation of errors, the uncertainty in each thickness determination was assumed to be 20%. This effect was reduced by using three different targets in the experiment and assuming the error in the target thickness to be due to statistical effects. This should be valid since any systematic error is largely compensated for by the calibration target whose thickness was determined in the same way.

Calibration of the spectrograph was achieved using the ^{92}Mo(^{12}C, ^{10}Be)^{94}Ru ($Q = -16.844 \pm 0.014$ MeV) and ^{92}Mo(^{12}C, ^{9}Be)^{95}Ru ($Q = -14.703 \pm 0.013$

[1] Current address: Argonne National Laboratory, Argonne, IL 60439, USA.
[2] Permanent address: Institute de Physique Nucléaire, 91406, Orsay, France.

THE ^{26}Mg(p, n)^{26}Al REACTION AND THE ENERGY DEPENDENCE OF THE SPIN–ISOSPIN EFFECTIVE INTERACTION ☆

W.A. STERRENBURG
Cyclotron Laboratory, Michigan State University, East Lansing, MI 48824, USA

Sam M. AUSTIN
Département de Physique Nucléaire/ME, CEN Saclay, 91190 Gif-sur-Yvette, France
and Cyclotron Laboratory and Physics Department, Michigan State University, East Lansing, MI 48824, USA

and

U.E.P. BERG and R. DeVITO
Cyclotron Laboratory and Physics Department, Michigan State University, East Lansing, MI 48824, USA

Received 6 February 1980

Cross sections for the ^{26}Mg(p, n)^{26}Al reaction leading to the isobaric analog state and to low-lying 1^+, $T = 0$ states have been measured at bombarding energies of 24.6, 35.0 and 45.0 MeV. Several different approaches have been used to obtain values of the spin-flip ($V_{\sigma\tau}$) and no spin-flip (V_τ) parts of the effective interaction. The ratio $V_{\sigma\tau}/V_\tau$ increases with increasing energy between 25 and 45 MeV. Extracted values of $V_{\sigma\tau}$ are somewhat larger than those obtained from lighter nuclei.

There are strong indications [1] that giant Gamow–Teller strength has been observed in (p, n) reactions at bombarding energies above 25 MeV. To draw quantitative conclusions about the intrinsic strength of the observed transitions, however, requires a priori knowledge of $V_{\sigma\tau}(\sigma_1 \cdot \sigma_2)(\tau_1 \cdot \tau_2)$, the part of the effective interaction responsible for reactions such as these which transfer both spin and isospin. Unfortunately little reliable information is available. Empirical values of $V_{\sigma\tau}$ have been obtained [2] from reactions on very light nuclei, mostly $A = 6, 7$, but suffer from the usual uncertainties involved in distorted-wave-Born-approximation (DWBA) analyses for such light nuclei. Theoretical effective interactions are available [3,4], but their spin–isospin-dependent parts do not appear to be very accurate [4]. The measurements described in this letter are a first attempt to obtain information about $V_{\sigma\tau}$ from a nucleus sufficiently heavy and well understood to permit a reliable DWBA analysis of the cross sections.

Cross sections for the ^{26}Mg(p, n)^{26}Al reaction, leading to the 0^+, $T = 1$ isobaric analog state at 0.23 MeV, and to 1^+, $T = 0$ states at 1.06 and 1.85 MeV, were measured at 24.6, 35.0 and 45.0 MeV. Two sorts of analyses have been made, one involving a straightforward application of the DWBA and the other a simple approximation based on the relationship of the β-decay and (p, n) operators. Values of $V_{\sigma\tau}$ and of the no-spin-transfer interaction, $V_\tau \tau_1 \cdot \tau_2$, obtained from these analyses show that the ratio $V_{\sigma\tau}/V_\tau$ increases as the energy increases from 25 to 45 MeV. One concludes that the (p, n) reaction at 35 MeV and above will be a powerful tool for identifying spin transfer strength in nuclei.

The experiment utilized the beam-swinger time-of-flight system at Michigan State University [5]. Protons from the MSU cyclotron bombarded a 5.0 mg/cm^2 thick ^{26}Mg target enriched to 99.5% in ^{26}Mg.

☆ Supported in part by the U.S. National Science Foundation.
† Present address: Institut für Kernphysik, Justus-Liebig-Universität, D-6300 Giessen, Germany.

EFFECTS OF NON-LINEAR TERMS IN THE WEINBERG LAGRANGIAN ON PION–NUCLEUS SCATTERING AND NUCLEAR BINDING ☆

H. McMANUS and D.O. RISKA
Department of Physics, Michigan State University, East Lansing, MI 48824, USA

Received 23 January 1980
Revised manuscript received 4 March 1980

The non-linear terms in the Weinberg chiral lagrangian for pion–nucleon systems give large individual contributions to the S-wave pion–nucleus optical potential, but strong cancellations leave only an insignificant net contribution. The cancellation is exact in the zero range limit. These terms also give rise to 4-nucleon interactions which however only marginally affect nuclear binding.

Recently considerable attention has been given to the nuclear implications of the non-linear terms in chiral lagrangians for the pion–nucleon systems. The lowest order non-linear terms contribute to the pion–nucleus interaction by the pion exchange diagrams in fig. 1. Considering the contributions of these diagrams to the pion deuteron scattering length, Robilotta and Wilkin [1], employing the most general chiral lagrangian for the pion and nucleon field consistent with current algebra and PCAC given by Olsson and Turner [2], found however an almost complete cancellation between the individual contributions and thus but a very small net effect. Miller and Noble [3], in a work on the application of $\sigma + \omega$ meson model to the pion–nucleus interaction, have pointed out that these non-linear terms could contribute to the real part of the S-wave pion–nucleus potential. We shall here show, that within the framework of the Weinberg's lagrangian [4], which is the one best suited for this problem [5], a cancellation (similar to that found by Wilkin and Robilotta) also occurs for the S-wave optical potential.

In order to construct the optical potential contribution due to the diagrams in fig. 1 we need the following interactions, obtained by expanding the relevant terms in Weinberg's lagrangian [4]:

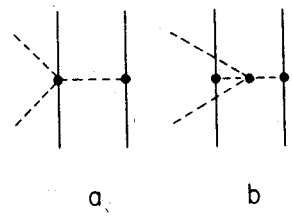

Fig. 1. Pion exchange contributions to the pion–nucleus interaction caused by the lowest order non-linear terms in the chiral lagrangians. The dashed lines indicate pions.

$$\mathcal{L}_{\pi NN} = -i(f/\mu)\bar{N}\gamma_\mu\gamma_5\boldsymbol{\tau}\cdot\partial_\mu\boldsymbol{\pi}N\,,$$

$$\mathcal{L}_{\pi\pi\pi NN} = i(f/\mu)^3\bar{N}\gamma_\mu\gamma_5\boldsymbol{\pi}^2\boldsymbol{\tau}\cdot\partial_\mu\boldsymbol{\pi}N\,, \qquad (1)$$

$$\mathcal{L}_{\pi\pi\pi\pi} = (f/\mu)^2\boldsymbol{\pi}^2(\partial_\mu\boldsymbol{\pi}\cdot\partial_\mu\boldsymbol{\pi} + \tfrac{1}{2}\mu^2\boldsymbol{\pi}^2)\,.$$

Here f is the pseudovector πN coupling constant ($f^2/4\pi \approx 0.08$), μ the pion mass and N the nucleon and $\boldsymbol{\pi}$ the isovector pion field operator. In (1) we have set $g_V/g_A = 1$. The scattering amplitudes for the diagrams in fig. 1 are now readily constructed. For the S-wave optical potential we only need consider the static isoscalar spin-scalar part of the amplitudes.

☆ Research supported in part by the National Science Foundation.

ASYMPTOTIC FORM OF MONOPOLE VIBRATIONS

F.E. SERR, G.F. BERTSCH and J. BORYSOWICZ
Cyclotron Laboratory and Physics Department, Michigan State University, East Lansing, MI 48824, USA

Received 11 February 1980
Revised manuscript received 19 March 1980

The velocity field for monopole vibrations of large nuclear systems is shown to obey the classical equations for an elastic medium, rather than a fluid. In the surface the velocity field becomes an increasing exponential. For ^{208}Pb, these effects combine to give motion similar to the Tassie model.

Highly collective nuclear states, such as the giant monopole vibration, are often described in fluid dynamical terms [1,2]. It is also possible to cast microscopic calculations in forms which give meanings to many classical continuum variables [3–7]. The liquid drop description is commonly thought to be correct for such macroscopic variables, at least in the limit of large nuclei. However, the Tassie model [8–10] also seems to give good results for heavy nuclei. For the monopole, the Tassie model is a simple radial scaling of the wavefunctions. These two models yield quite different forms for the velocity field of the collective motion, especially near the surface. Detailed microscopic calculations of the monopole vibration in ^{208}Pb [11] give a velocity field with an intermediate form. (See fig. 1.) A clear determination of the motion in the large A limit, with no assumptions on the form of the exciting field, has not been made. This is important if monopole vibrations are used to specify properties of nuclear matter. There also remains the question of whether ^{208}Pb is large enough to exhibit this asymptotic behavior.

We show below that the velocity field for monopole vibrations of large spherical nuclear systems is neither liquid drop nor Tassie. The motion of the bulk of the particles is well described by the classical equations for vibrations of an elastic medium, rather than a fluid. The surface boundary condition for the velocity field is an increasing exponential. We express this in terms of binding energies of the ground and excited states.

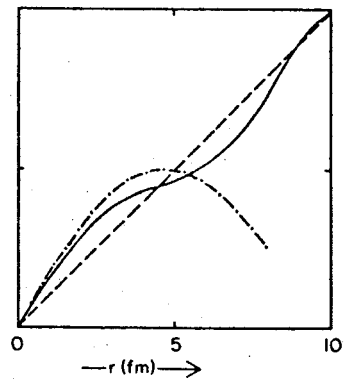

Fig. 1. Velocity fields for monopole vibration of ^{208}Pb: solid line, full RPA calculation (from ref. [11]); dashed line, Tassie model ($u_r \propto r$); dash-dot line, liquid drop model ($u_r \propto j_1(\pi r/R)$).

For systems as small as ^{208}Pb, this surface condition still masks the bulk behavior.

We have made variational calculations of the velocity field of the monopole vibration in both Bose and Fermi systems with density-dependent interactions. The RPA theory for a coherent collective state has previously been expressed in terms of the velocity field [3]. The derivation starts with the time-dependent Hartree–Fock formalism, then assumes small amplitude harmonic motion. The velocity field is then a small displacement vector, $u(r) \equiv \nabla\Phi(r)$, with a harmonic time dependence. Further assumption of a single velocity field for all the particles leads to a compact expression for the frequency

CORE-POLARIZATION EFFECTS ON THE MAGNETIC TRANSITIONS IN THE ^{208}Pb REGION

I. HAMAMOTO [1,2]
Center for Theoretical Physics, Laboratory for Nuclear Science, and Department of Physics, MIT, Cambridge, MA 02139, USA

J. LICHTENSTADT [2]
Bates Linear Accelerator Center, Laboratory for Nuclear Science, and Department of Physics, MIT, Cambridge, MA 02139, USA

and

G.F. BERTSCH [3]
Department of Physics and Cyclotron Laboratory, Michigan State University, East Lansing, MI 48824, USA

Received 25 February 1980

We show that there is a reduction of the magnetic transition strength at high momentum transfer due to core polarization. This accounts substantially for the observed reduction of 50% of the $J^\pi = 12^-$ and 14^- transitions in ^{208}Pb. The core polarization does not affect the shape of the high J form factors in the vicinity of their main peaks. However, a significant q-dependent effect is predicted for the ground state M1 moment of ^{207}Pb.

High spin states with unnatural parity of $J^\pi = 14^-$(6.74 MeV) and 12^-(6.43 and 7.06 MeV) have been measured recently in inelastic electron scattering measurements indicating significant reduction from the single particle–hole predictions [1]. The observed strengths around the first maximum of the form factors were only about 50% of the predictions from the $\nu(1j_{15/2}, 1i_{13/2}^{-1})14^-, 12^-$ and the $\pi(1i_{13/2}, 1h_{11/2}^{-1})12^-$ configurations. The purpose of the present letter is to estimate the core-polarization effect on these magnetic form factors, by using the technique of integrating the Schrödinger equation in the radial coordinate space [‡1,2].

Since in each of these high spin states one definite particle–hole configuration (denoted by p_0–h_0) is supposed to be the overwhelmingly predominant component, we calculate the contributions from the graphs shown in figs. 1a and 1b. The complete sum over particle–hole configurations p, h may be performed easily if the residual interaction is approximated by a delta function. We obtain the following inhomogeneous equation [2–4] for the perturbed particle wavefunction, $X_{ph}(r)$,

$$\left\{\frac{\hbar^2}{2m}\left(-\frac{d^2}{dr^2}+\frac{l_p(l_p+1)}{r^2}\right)+V(r)-(E+\epsilon_h)\right\} rX_{ph}(r)$$
$$= -rR_{h_0}(r)R_h(r)R_{p_0}(r)\langle(Y_{l_p}\tfrac{1}{2})^{j_p}(Y_{l_h}\tfrac{1}{2})^{j_h}|v\delta(\Omega_1-\Omega_2)|(Y_{l_{p_0}}\tfrac{1}{2})^{j_{p_0}}(Y_{l_{h_0}}\tfrac{1}{2})^{j_{h_0}}\rangle_J. \quad (1)$$

[1] Address after September 1980: Nordita, Copenhagen, Denmark.
[2] Supported in part by US DOE, contract No. EY-76-C-02-3069.
[3] Supported in part by the National Science Foundation.
[‡1] This formalism was taken from Buck and Hill [2]. See also Hamamoto [3].
[‡2] It is useful both formally and numerically to define a Green's function here. See Shlomo and Bertsch [4].

Octupole states in ^{63}Cu and the weak-coupling picture

Y. Iwasaki, G. M. Crawley, R. G. Markham,* J. E. Finck,† and J. H. Kim
Cyclotron Laboratory, Michigan State University, East Lansing, Michigan 48824
(Received 5 April 1979)

A high-resolution experiment of proton inelastic scattering by ^{63}Cu at E_p = 40 MeV has resolved three octupole states at E_x = 3.81, 3.84, and 3.89 MeV for the first time, thus showing the existence of seven strong octupole states in ^{63}Cu. This finding is direct evidence that the traditional simple weak-coupling model in terms of one quartet $2p_{3/2} \otimes 3_1^-$ is inadequate for the octupole core-excited states in ^{63}Cu. This is not evidence, however, that the weak-coupling picture in general is incorrect for the octupole states in ^{63}Cu. It is shown that to be consistent with the present experimental data, the weak-coupling picture for the octupole states requires a ground-state wave function substantially different from the ground-state wave function of the conventional particle-core-coupling model.

[NUCLEAR REACTIONS ^{63}Cu(p,p'), E_p = 40 MeV, strong octupole transitions, resolved new levels. Measured differential cross sections. Discussion in terms of the weak-coupling picture for the octupole states.]

In the particle-core-coupling picture, the nucleus ^{63}Cu consists of a single proton coupled to the proton-closed-shell nucleus ^{62}Ni, which is called the core.[1] Inelastic scattering is known to be an effective means of selectively exciting collective degrees of freedom of the core.[2-5] We have studied the inelastic scattering of protons by ^{63}Cu at E_p = 40 MeV, and have found seven strong octupole transitions leading to states at E_x = 2.51, 3.32, 3.48, 3.72, 3.81, 3.84, and 3.89 MeV in ^{63}Cu. The three states at E_x = 3.81, 3.84, and 3.89 MeV have been resolved for the first time. Since previous experiments using (α,α'),[3] (p,p'),[4] and (e,e')[5] reactions did not resolve these three states, up till now only five strong octupole states have been reported. Four of them have been suggested to be members of a quartet that arises from the coupling of the $2p_{3/2}$ proton orbital with the octupole state of the core (the 3_1^- state at E_x = 3.75 MeV in ^{62}Ni)[1,6] in accordance with the excited-core model.[2,3,7] The remaining one at E_x = 2.51 MeV is a predominantly single-particle state containing the $1g_{9/2}$ proton orbital with a large amplitude.[8,9] The strongly enhanced octupole transition to the state is a puzzle for which an explanation has been offered recently.[6] There are, however, two more strong octupole states. This new finding corrects the experimental information upon which the traditional weak-coupling excited-core model[1,6] has been based.

Fig. 1 shows part of the ^{63}Cu(p,p') spectrum at a laboratory angle of 24° measured in the Enge split-pole magnetic spectrograph using a delay-line counter.[10] The overall energy resolution is about 20 keV. The seven octupole states are indicated by arrows. Fig. 2 shows the differential cross sections for the transitions to the octupole states. All the angular distributions have the characteristic L = 3 shape.[11] Fig. 3 shows that there is no ambiguity in distinguishing between the L = 2, 3, and 4 angular distributions. The third column of Table I gives the relative cross sections for the octupole transitions.

The existence of two extra octupole states is direct evidence that the simple weak-coupling model in terms of the $2p_{3/2} \otimes 3_1^-$ quartet[1,3,6] is inadequate. This raises the question whether the weak-coupling picture in general is incompatible with the present experimental data. If the weak-coupling picture is assumed for the six higher octupole states, these states are excited in the (p,p') reaction by a simple core-excitation mechanism. In addition to the quartet of the simple weak-coupling model,[1,3,6] we are naturally led to consider a doublet of states with $J^\pi = 5/2^-$ and $7/2^-$ arising from the weak coupling of the $2p_{1/2}$ proton orbital with the 3_1^- state of the core, since two additional states have been found. These doublet states can be excited only by the octupole transition from the 2_1^+ state to the 3_1^- state of the core, since the $2p_{1/2}$ orbital is occupied in the ground state of ^{63}Cu only as a result of the coupling with the lowest quadrupole state of the core, i.e. only in the form $[2p_{1/2} \otimes 2_1^+(\text{core})]_{3/2}$. Let us denote the reduced

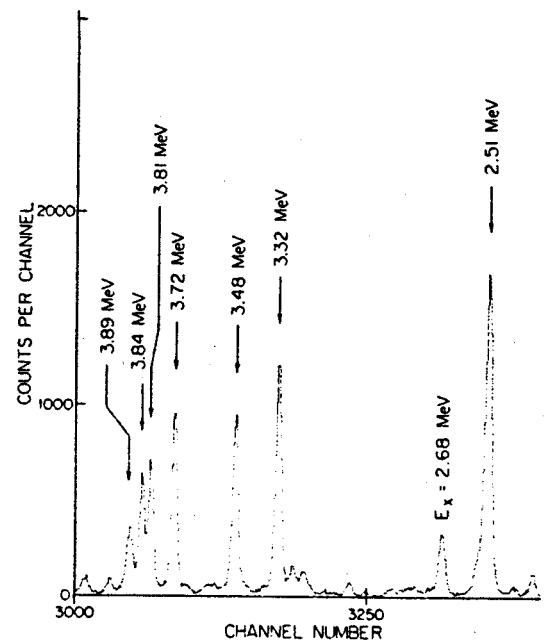

FIG. 1. Part of the ^{63}Cu(p,p')^{63}Cu spectrum at 24° lab. Arrows indicate octupole states. Overall energy resolution is about 20 keV. The state at E_x = 2.68 MeV is excited by a hexadecapole transition (see Fig. 3).

^{194,196,198}Pt(p,t) reactions at 35 MeV

P. T. Deason, C. H. King,* T. L. Khoo,† J. A. Nolen, Jr., and F. M. Bernthal
Departments of Chemistry and Physics and Cyclotron Laboratory, Michigan State University, East Lansing, Michigan 48824
(Received 6 April 1979)

The ^{194,196,198}Pt(p,t) reactions have been studied at a proton energy of 35 MeV using nuclear emulsion plates and a high-resolution position-sensitive proportional counter. Fifty states were observed in ^{194}Pt and ^{196}Pt and sixty-four in ^{192}Pt, many for the first time. Angular distributions were measured for many of these levels from 7° to 60° and the results were compared with zero-range distorted wave Born approximation calculations. Several new J^π assignments were made using distorted wave Born approximation and empirical shapes of transitions to well-known levels in Pt and Pb. No new levels, in particular, no new 0^+ levels, were seen below 1.5 MeV excitation. A new 0^+ level at 1.628 MeV was found in ^{192}Pt, and new levels tentatively assigned to be 4^+ were seen in all three final nuclei near 1.9 MeV with 15% of the ground state strength at 7° in the ^{196,198}Pt(p,t) reactions. Enhancement factors were calculated for simple two-neutron pickup configurations. A comparison is made between experimental (p,t) strengths and those calculated in the O(6) limit of the interacting boson approximation model for $L = 0, 2$ transitions.

[NUCLEAR REACTIONS ^{194}Pt(p,t), ^{196}Pt(p,t), and ^{198}Pt(p,t), E_p = 35 MeV; measured $\sigma(E_t, \theta)$; deduced energies, J^π, and strengths; DWBA calculations, comparison with experiment; enhancement factors. Enriched targets, 7 keV resolution (plates); interacting boson approximation model.]

I. INTRODUCTION

The Pt isotopes lie in a transitional region between well-deformed rare-earth nuclei and the spherical nuclei near doubly magic ^{208}Pb. Since the Pt nuclei are not well described by either of the simple Bohr-Mottelson collective-model limits, the symmetric rotor or the harmonic vibrator, they provide a valuable testing ground for current models of collective nuclear motion.

It has been known for several years that a transition from prolate to oblate shapes occurs among the heavier Os and the lighter Pt nuclides.[1,2] For the heavier Pt nuclides ($^{192-198}$Pt) the quadrupole deformation parameter, β, has a value[3,4] of approximately 0.15, or about one half the value determined for the well-deformed rare earth nuclei and consequently these Pt isotopes exhibit few rotational features. Some of the features of the lowest energy levels of these nuclides can be interpreted in terms of a harmonic vibrator. However, a notable problem with this picture is the lack of a candidate for the 0^+ member of the 2-phonon triplet. Moreover, the platinum isotopes are farther away from closed shells than those nuclei for which vibrational models have been applied most successfully.

Because of the difficulty with harmonic vibrational models, various other collective models have been tried, such as the γ-unstable[5] or the asymmetric rotor[6] models. These models seem appropriate here because of the lack of low-lying excited 0^+ levels. The asymmetric rotor model in particular has recently enjoyed some success for odd-A nuclides in this region,[7-11] but neither this nor any of the standard limits of the collective model seem capable of describing the structure of the even-even nuclides. As a result, several attempts[12-14] have been made to treat this region by solving the full collective Hamiltonian, beginning with the pioneering work of Kumar and Baranger in which the parameters of the Hamiltonian were determined by using the pairing-plus-quadrupole model. These more complete treatments of the collective model have had considerably more success in accounting for the low-lying properties of the nuclides in the platinum-osmium region using a potential energy surface which implies a relatively γ-soft nucleus. Nevertheless, mathematical solutions for these models present formidable difficulties.

A simpler description of the nuclides in the platinum-osmium region has recently emerged from the interacting-boson approximation (IBA) model of Iachello and Arima.[15] In this model the nucleus is treated in terms of a set of bosons, one for each pair of neutrons or protons outside a closed shell. The bosons can be in either an $L = 0$ or $L = 2$ state and are allowed to interact. The most general Hamiltonian describing such a system possesses an SU(6) group symmetry. Particularly simple descriptions are possible when the Hamiltonian is symmetric with respect to subgroups of SU(6). The SU(5) subgroup, for example, corresponds approximately to the vibrational limit of the collective model, and SU(3) to the rotational limit. Another important subgroup of SU(6) is O(6), and Cizewski et al.[16] have shown that this limit accounts for most of the energy and decay properties of all positive parity levels below the pairing gap for ^{196}Pt. In fact, the structure of ^{196}Pt and most of the lighter mass even-even Os and Pt nuclides can be understood[16] by adding a small but gradually increasing symmetry-breaking term to the Hamiltonian as one goes farther away from the O(6) limit.

The majority of the experimental information on the heavier Pt isotopes has come from γ-ray studies following the $\varepsilon, \beta^\pm$ decay of Au and Ir isotopes.[17-22] There have also been several publications on γ-decay following neutron capture.[23-26] More recently the nature of the high-spin levels of the platinum nuclides up to spin 20^+ has been studied by (α,$xn\gamma$) in-beam γ-ray spectroscopy.[8,27-29]

There have been numerous inelastic scattering experiments[13,30-33] performed on the Pt nuclides, primarily by Coulomb excitation of the first 2^+ states. The bulk of the transfer reaction data is from one-neutron transfer studies of the odd platinum nuclei,[34-38] with the exception of an investigation of the ^{196}Pt(p,t) reaction in a search for strong $L = 0$ transitions in heavier nuclei.[39]

The present high-resolution (p,t) reaction study utilized a 35 MeV proton beam and was undertaken as a search for low-lying 0^+ levels in the even-even platinum nuclides, ^{192,194,196}Pt. The (p,t) reaction was chosen for the distinctive, diffraction-like shapes of the $L = 0$ transfers.

PHYSICAL REVIEW C VOLUME 20, NUMBER 3 SEPTEMBER 1979

Decay of ^{201}Pb

R. E. Doebler* and Wm. C. McHarris

Department of Chemistry, Cyclotron Laboratory, and Department of Physics, Michigan State University, East Lansing, Michigan 48824

W. H. Kelly

Cyclotron Laboratory and Department of Physics, Michigan State University, East Lansing, Michigan 48824

(Received 27 September 1978)

γ rays emitted in the decay of 9.4-h ^{201}Pb were studied with Ge(Li) and NaI(Tl) detectors in singles, anti-Compton, anticoincidence, and integral coincidence configurations. The construction of a consistent decay scheme including 66 of the 74 γ rays observed in the decay of ^{201}Pb was also aided by a two-dimensional γ-γ coincidence experiment of 4096 × 4096 channels using two Ge(Li) detectors. The proposed levels in ^{201}Tl lie at 0, 331.15, 692.40, 1098.4, 1134.8, 1157.4, 1238.8, 1277.1, 1290.0, 1330.4, 1401.2, 1420.0, 1445.8, 1479.9, 1575.1, 1617.4, 1639.5, 1672.0, and 1755.3 keV with possible additional levels at 1550.5 and 1712.5 keV. Using existing conversion-electron data, conversion coefficients were calculated and multipolarity assignments proposed for 25 transitions. Based on these multipolarities, photon branching ratios, and logft values, unique spin and parity assignments have been made for several states and limits placed on others. The resulting decay scheme is compared with recent theoretical calculations of level energies and γ transition probabilities, using the intermediate-coupling unified model.

[RADIOACTIVITY ^{201}Pb [from ^{203}Tl(p,3n) and ^{203}Tl(^{3}He,5n) ^{201}Bi $\xrightarrow{\varepsilon}$ ^{201}Pb]; measured E_γ, I_γ, α_K, α_L; deduced logft; ^{201}Tl deduced levels, J, π; Ge(Li) singles and γ-γ coincidence.]

I. INTRODUCTION

The neutron-deficient odd-mass Tl isotopes have been the subject of numerous theoretical investigations, the most recent being those of Covello and Sartoris,[1] Alaga and Ialongo,[2] and Azziz and Covello.[3] These recent calculations have been made using the intermediate-coupling unified model in which collective effects, treated as vibrations of the spherical core, are coupled more or less strongly to the single-particle states. Because the odd-mass Tl isotopes are only one proton removed from the Z = 82 closed shell and only a few neutrons from the N = 126 closed shell, they are an ideal choice for calculations using this model.

Since the level schemes of ^{207}Tl, ^{205}Tl, and ^{203}Tl obtained from radioactive decay are relatively simple and have been studied thoroughly, we have started our investigation of these isotopes with the states in ^{201}Tl populated by the decay of 9.4-h ^{201}Pb. In a forthcoming paper[4] we will present a study of states in ^{199}Tl populated by 90-min ^{199}Pb.

^{201}Pb was first reported in 1946 by Howland, Templeton, and Perlman[5] as a 5-h activity resulting from the reaction, ^{203}Tl(α,4n)^{201}Pb. In 1950 Neuman and Perlman[6] reported an 8 ± 2-h Pb activity as the daughter of both the 62-min and 2-h isomers of ^{201}Bi. In the following years the decay of ^{201}Pb was studied by numerous groups[7-11] using magnetic β-ray spectrometers for internal-conversion electron measurements and NaI(Tl) detectors for photons. The most recent and comprehensive of these studies was published by Aasa et al.[12] in 1964. Using an iron-yoke double-focusing β spectrometer, they assigned 32 γ transitions to the decay of ^{201}Pb and proposed a decay scheme containing 10 excited levels. However, their decay scheme was far from complete and contained many uncertainties, which prompted the present investigation.

II. SOURCE PREPARATION

A. ^{203}Tl(p,3n)^{201}Pb

Most of the ^{201}Pb sources used in this study were produced by bombarding natural Tl foils (70% ^{205}Tl, 29.5% ^{203}Tl) with 27-MeV protons from the Michigan State University sector-focused cyclotron to induce the reaction, ^{203}Tl(p,3n)^{201}Pb. A typical bombardment time was ≈1 hr.

The principal contaminants in these sources were 52-h ^{203}Pb, 3.6-h ^{202}Pb^m, and 67-min ^{204}Pb^m. ^{204}Pb^m was essentially eliminated and ^{202}Pb^m considerably reduced in these sources by aging them for 12 to 18 h prior to counting. 52-h ^{203}Pb was by far the most significant contaminant in these sources. Actually, ^{203}Pb usually accounted for more of the source activity than ^{201}Pb and its strength was enhanced with respect to 9.4-h ^{201}Pb by aging the sources. Fortunately, the decay of ^{203}Pb has been well studied and only three γ rays are emitted in its decay,[13] which were confirmed again in the present study. The biggest problem caused by this contaminant was to increase the Compton background for energies below 279 keV, thereby making it more difficult to observe weak γ rays in this region. Toward the end of our experiments we did make one source using enriched ^{203}Tl (70% ^{203}Tl, obtained from Oak Ridge National Laboratory), and the ^{203}Pb activity in this source was substantially reduced.

Simply aging the sources, however, did not completely eliminate the problem of source purity, for the Tl daughters of ^{201}Pb and ^{202}Pb^m, 73-h ^{201}Tl and 12-d ^{202}Tl, are also γ-ray emitters. Therefore, we always performed a chemical separation of the Pb activity from the Tl target at the end of the aging period prior to counting. The Tl target was dissolved in the smallest

$^{17}O(^3He,p)^{19}F$ and the structure of ^{19}F

J. N. Bishop,* L. R. Medsker,† and H. T. Fortune
Physics Department, University of Pennsylvania, Philadelphia, Pennsylvania 19104

B. H. Wildenthal
Cyclotron Laboratory, Michigan State University, East Lansing, Michigan 48824

(Received 12 January 1979)

Angular distributions have been measured for 18 levels of ^{19}F populated in the reaction $^{17}O(^3He,p)$ at a bombarding energy of 18 MeV. Within the experimental resolution of 28 keV all levels below 5.7 MeV were observed. Nine states were excited with peak differential cross sections greater than 50 μb/sr, all others had maximum cross sections of less than 12 μb/sr. Eight of the nine strong levels are easily identifiable with $(sd)^3$ shell-model states. The ninth is the state at 5.11 MeV, previously assigned $J^\pi = 5/2^-$, but suggested by the present results to have positive parity. Angular distributions were analyzed with the distorted-wave Born approximation. For the strong states, transfer amplitudes were taken from an $(sd)^3$ shell-model calculation. Agreement in both shape and magnitude is good. Negative-parity hole states and positive-parity core-excited states are very weakly populated, but in many cases, their angular distributions are also well fitted with admixtures of the allowed L values.

[NUCLEAR REACTION $^{17}O(^3He,p)$, $E=18.0$ MeV; ^{19}F deduced levels, L, Π. DWBA analysis.]

I. INTRODUCTION

In the $^{18}O(^3He,p)^{20}F$ reaction,[1] a comparison of measured angular distributions with those predicted using microscopic wave functions provided an excellent means of identifying the $(sd)^4$ states in ^{20}F. The present report concerns a similar investigation of the reaction $^{17}O(^3He,p)^{19}F$. The nucleus ^{19}F has been studied with a variety of reactions, including $^{18}O(^3He,d)$,[2,3] $^{18}O(d,n)$,[4] $^{16}O(\alpha,p)$,[5] $^{16}O(^6Li,^3He)$,[6] $^{16}O(^7Li,\alpha)$,[7] $^{15}N(^7Li,t)$,[8] $^{17}O(\alpha,d)$,[9] $^{15}N(\alpha,\gamma)$,[10,11] $^{19}F(p,p')$,[12] and $^{19}F(\alpha,\alpha')$.[13] All the

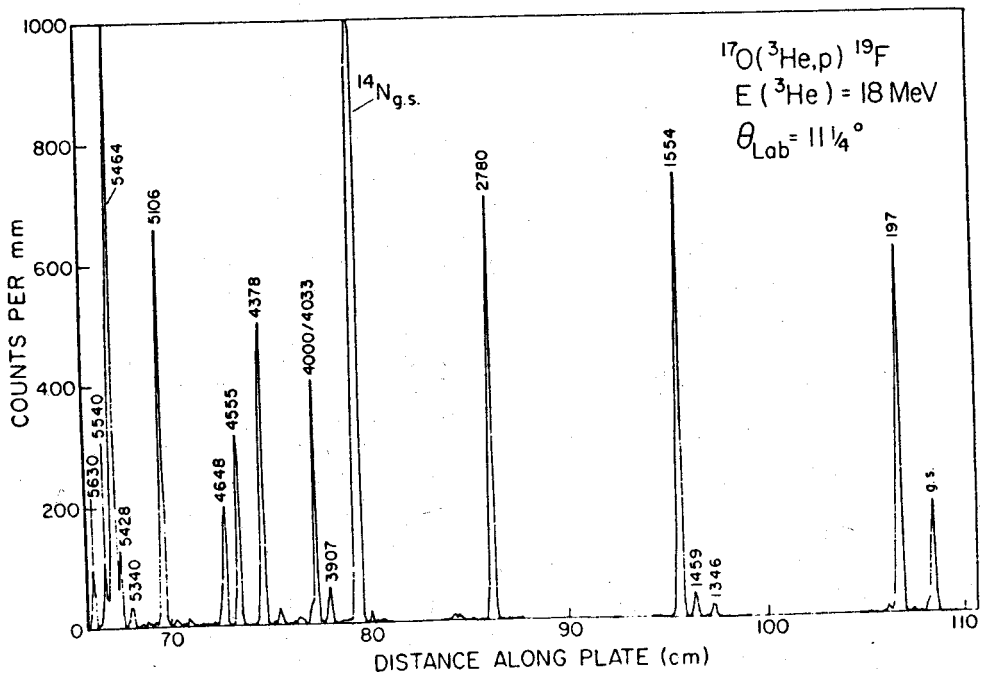

FIG. 1. Spectrum of the $^{17}O(^3He,p)^{19}F$ reaction at a bombarding energy of 18 MeV and a laboratory angle of 11.25°. Peaks are labeled with energies from a previous compilation. Excitation energies measured in the present work are listed in Table I. Small unidentified peaks arise from the $(^3He,p)$ reaction on other isotopes of oxygen.

PHYSICAL REVIEW C VOLUME 20, NUMBER 5 NOVEMBER 1979

$^{14}C(p,n)^{14}N$ and the isovector tensor component of the effective two-nucleon interaction

R. R. Doering
Department of Physics, University of Virginia, Charlottesville, Virginia 22901
and Cyclotron Laboratory, Michigan State University, East Lansing, Michigan 48824

T. N. Taddeucci
Department of Physics, University of Virginia, Charlottesville, Virginia 22901

Aaron Galonsky and D. M. Patterson*
Cyclotron Laboratory, Michigan State University, East Lansing, Michigan 48824
(Received 13 November 1978; revised manuscript received 6 June 1979)

Angular distributions have been measured for the $^{14}C(p,n)^{14}N$(0.0 and 3.95 MeV) reactions at $E_p = 35$ MeV. The differential cross sections for the two 1^+ states (0.0 and 3.95 MeV) have been compared with antisymmetrized distorted-wave Born-approximation calculations based on phenomenological and realistic effective two-nucleon interactions. In contrast to recent analyses of spin-sensitive measurements, the $^{14}C(p,n)^{14}N$(g.s.) data definitely favor the inclusion of an isovector tensor interaction.

[NUCLEAR REACTIONS $^{14}C(p,n)^{14}N$, $E = 35$ MeV; measured $\sigma(\theta)$. DWBA analysis, deduced tensor force.]

Previous experiments have turned up conflicting evidence for the necessity of including tensor components in the effective nucleon-nucleon interaction. In several studies,[1-4] differential cross sections have been shown to favor the presence of a tensor force of roughly the same magnitude (relative to the central terms) as that present in the free nucleon-nucleon interaction. On the other hand, recent measurements[5-7] of spin-flip and polarization have not been well fitted with its inclusion.

The reaction $^{14}C(p,n)^{14}N$(g.s.) is of special interest for studying this problem because of its predicted[8] sensitivity to the tensor force. The present work differs from previous studies of this reaction in two significant respects. First, knock-out exchange amplitudes have been incorporated in our distorted-wave Born approximation (DWBA) calculations. In addition, our bombarding energy ($E_p = 35$ MeV) is higher: this should further enhance the relevance of the DWBA analysis. In contrast to the conclusion based on spin-sensitive measurements,[5-7] we find that a tensor force of significant magnitude must be included to explain our data.

Our $^{14}C(p,n)^{14}N$ data were taken with a neutron time-of-flight system[9] at the Michigan State University Cyclotron Laboratory. Angular distributions from 10° to 160° in the lab were measured for the states of ^{14}N at 0.0 MeV (1^+) and 3.95 MeV (1^+). The ^{14}C target was prepared with the technique described in Ref. 10. The absolute error in the normalization of our cross sections is estimated to be less than 20%.

The effective nucleon-nucleon interaction can be represented in a local, phenomenological form as

$$V_{eff} = [V_0 + V_\sigma \vec{\sigma}_i \cdot \vec{\sigma}_p + V_\tau \vec{\tau}_i \cdot \vec{\tau}_p + V_{\sigma\tau} \vec{\sigma}_i \cdot \vec{\sigma}_p \vec{\tau}_i \cdot \vec{\tau}_p + (V_{LS} + V_{LS\tau} \vec{\tau}_i \cdot \vec{\tau}_p) \vec{L} \cdot \vec{S} + (V_T + V_{T\tau} \vec{\tau}_i \cdot \vec{\tau}_p) S_{ip} r^2] e^{-r/a} (r/a)^{-1}, \quad (1)$$

where S_{ip} is the tensor operator

$$S_{ip} = 3\vec{\sigma}_i \cdot \hat{r} \vec{\sigma}_p \cdot \hat{r} - \vec{\sigma}_i \cdot \vec{\sigma}_p .$$

For a $0^- - 1^+$, $\Delta T = 1$ transition, the direct part of the transition amplitude will be mediated by the $V_{\sigma\tau}$, $V_{LS\tau}$, and $V_{T\tau}$ terms. The central $V_{\sigma\tau}$ term allows orbital angular momentum transfers of $L' = L = 0,2$, where L' is the angular momentum transferred to the nucleus and L is that transferred to the projectile. It has been shown,[8] however, that for $L = 0$ the contribution from the central isovector spin-flip term is nearly proportional to the Gamow-Teller β-decay matrix element, which is strongly suppressed for $^{14}C - {}^{14}N$ (g.s.). Thus, the contribution from this term to $^{14}C(p,n)^{14}N$(g.s.) will be primarily $L = 2$. The spin-orbit contribution, because of parity considerations, will also be mostly $L = 2$. The tensor force, which is noncentral, allows angular momentum transfers to the projectile and nucleus to differ by two units, i.e., $L' = L, L \pm 2$.[11] The $L' = 0$ contributions will be inhibited, but the $L' = 2$ nuclear multipole will enter into both the $L = 0$ and $L = 2$ amplitudes. Thus, owing to the fortuitous suppression of the normally dominant $L = 0$ central-

^{20}O from ^{18}O(t,p)

S. LaFrance,* H. T. Fortune, S. Mordechai,* M. E. Cobern,† G. E. Moore,‡ and R. Middleton
Physics Department, University of Pennsylvania, Philadelphia, Pennsylvania 19104

W. Chung and B. H. Wildenthal
Cyclotron Laboratory, Michigan State University, East Lansing, Michigan 48823
(Received 2 July 1979)

We have investigated the reaction ^{18}O(t,p)^{20}O using enriched (96.6%) ^{18}O gas in a rotating gas cell and a multiangle spectrograph. Twenty-two angular distributions were measured for levels up to 10.2 MeV. Results are compared with predictions of a recent shell-model calculation.

[NUCLEAR REACTIONS ^{18}O(t,p), E_t = 15.0 MeV; measured $\sigma(E_p,\theta)$. ^{20}O deduced levels, L, π, J. DWBA analysis. Comparison with shell and weak-coupling models. Enriched gas target.]

I. INTRODUCTION

We have used the ^{18}O(t,p)^{20}O reaction to investigate the structure of ^{20}O. Data from this reaction for a few low-lying levels have been published previously.[1-3] Positive-parity states in ^{20}O are expected to be of two types: (1) ordinary shell-model states of $(sd)^4$ character—four neutrons outside an ^{16}O core, and (2) core-excited states, most probably of the type $(sd)^6(1p)^{-2}$, i.e., six-particle–two-hole. If the two types do not mix, then type 2 states can be populated in ^{18}O(t,p) only through core excitation in ^{18}O (g.s.).

Negative-parity levels will be mixtures of $(sd)^5(1p)^1$ and $(sd)^3(fp)$ configurations, but should be weak below about 7–8-MeV excitation.

A recent shell-model calculation[4] for nuclei throughout the sd shell has provided excellent agreement with energies and other observables, especially for nuclei near the ends of the shell. Two-particle transfer amplitudes from that work have been used in the present analysis. Figure 1 depicts the expected positions of the various types of states.

II. EXPERIMENTAL PROCEDURE AND RESULTS

A 15-MeV triton beam (current ~1 μA) bombarded a rotating gas cell[5] containing ^{18}O gas (enrichment 96.6%) at a pressure of 30 Torr. Protons exited through a 230-μg·cm^{-2} Al window, were momentum analyzed in a multiangle spectrograph and recorded in nuclear emulsions.

Data were recorded in steps of 7.5° (lab) beginning at 7.5°. A proton spectrum is displayed in Fig. 2. The only noticeable impurity peaks are from the (t,p) reaction on ^{16}O and ^{2}H. The broad bumps near 1- and 3-MeV excitations are not real peaks, but arise from the structure of the gas-cell supports. Peaks in Fig. 2 are labeled with their excitation energies, which are also listed in Table I, and compared with values from the literature.[2,6,7] These are averages of values obtained from peak positions at 7–10 angles, using the nominal beam energy and known magnet calibration. Twenty-two levels, or groups of levels, were observed below an excitation energy of 10.3 MeV. Their angular distributions are displayed in Figs. 3–5.

III. ANALYSIS AND DISCUSSION

Angular distributions were analyzed with the microscopic two-nucleon transfer option of the code DWUCK,[8] using transfer amplitudes from the shell-model calculation. Because of difficulties encountered in fitting the Q-value dependence of $L = 0$ angular-distribution shapes, two different sets of optical-model parameters[5,6,10] (Table II) were used in the analysis. Except for this difficulty, most of the fits are reasonably good.

For states below 6-MeV excitation, the present data confirm 0$^+$ assignments[6] for the g.s. and levels at 4.46 and 5.39 MeV, 2$^+$ assignments for levels at 1.67 and 4.07 MeV, and 4$^+$ for the 3.57-MeV state. Furthermore, we identify[2] levels at 4.85, 5.23, and 5.30 MeV as having $J^\pi = 4^+$, 2$^+$, and 2$^+$, respectively. The 0$^+$ level at 4.46 MeV and the 2$^+$ at 5.30 MeV have excitation energies and (t,p) cross sections consistent with expectation for the lowest $6p$-$2h$ states.[3] With the exception of these two states and a very weak state at 5.00 MeV all other states below 5.6 MeV appear to correspond rather well to $(sd)^4$ shell-model states. The strength and angular-distribution shape suggest unnatural parity

PHYSICAL REVIEW C VOLUME 20, NUMBER 6 DECEMBER 1979

(p,n) reaction for $89 < A < 130$ and an anomalous optical model potential for sub-Coulomb protons

C. H. Johnson
Oak Ridge National Laboratory, Oak Ridge, Tennessee 37830

A. Galonsky
Michigan State University, East Lansing, Michigan 48824

R. L. Kernell
Old Dominion University, Norfolk, Virginia 23508

(Received 14 May 1979)

The (p,n) cross sections were measured from about 2.5 to 5.8 MeV with about 100-keV target resolution for natural Pd, Ag, Cd, In, and Te and for ^{89}Y, ^{93}Nb, ^{103}Rh, ^{105,106,108,110}Pd, ^{107,109}Ag, ^{111,112,113,114,116}Cd, and ^{125,126,128,130}Te. Systematic uncertainties are about $\pm 2\%$ for ^{89}Y, ^{93}Nb, and the natural targets and about $\pm 4\%$ for the other nuclei. The isotopic $\sigma_{p,n}$ are fitted by adjustment in the depth W_D and diffuseness a_D of the surface imaginary part of a proton optical model potential (OMP) that was chosen previously to describe precision (p,n) data for isotopes of Sn. The diffuseness a_D is found to be nearly constant, about 0.4 fm, but the depth W_D shows a large and systematic A dependence. A study of the parameter space indicates that at least one OMP parameter must have a strong A dependence and that W_D is probably the only such single parameter that will suffice. The explanation of this anomaly is currently unclear.

NUCLEAR REACTIONS: Pd, Ag, Cd, In, Te, natural targets; and ^{89}Y, ^{93}Nb, ^{103}Rh, ^{105,106,108,110}Pd, ^{107,109}Ag, ^{111,112,113,114,116}Cd, ^{125,126,128,130}Te, enriched isotopic targets, $E = 2.5$ to 5.8 MeV, target resolution ~ 100 keV. Measured $\sigma_{p,n}$. Deduced optical model parameters.

INTRODUCTION

This work, which was summarized in a Letter,[1] is a study of medium weight nuclei in search of broad resonances in the proton strength function such as observed so far[2,3] only for the Sn isotopes. For the Sn isotopes Johnson *et al.*[2,3] measured precision (p,n) cross sections at sub-Coulomb energies (3 to 7 MeV), corrected for γ-ray and proton emission to obtain total reaction cross sections, fitted these cross sections with a proton optical model potential (OMP), and divided out the energy dependence of Coulomb penetration from the observed and fitted cross sections to reveal the nuclear effects. The resulting fitted curves for five isotopes from ^{117}Sn to ^{124}Sn are reproduced in Fig. 1(a). The ordinate $\langle S_p \rangle$, which is defined in Sec. IV D, is essentially the total reaction cross section divided by a $(2l+1)$-weighted sum of Coulomb penetration factors. Each curve exhibits a broad resonance; the peak energies shift systematically with increasing size of the nucleus. In the OMP these resonances result from the $3p$ state, which is quasibound by the combined real well and Coulomb potential and broadened by the imaginary potential.

It is reasonable to expect $3p$ resonances to be observed also in neighboring nuclei and to be described by the same OMP as for Sn, with minor adjustments in the parameters. To predict the curves in Fig. 1(a) for the nuclei studied here we have modified this OMP only by including conventional isospin and Coulomb dependences such that the depth of the real well increases 3% from ^{89}Y to ^{130}Te. (Section IV includes the parameters.) The predicted peak moves from 6.3 MeV for ^{89}Y to 5.3 MeV for ^{130}Te. This slow decrease demonstrates the nearly compensating effects of the increasing volume of the real nuclear well and the increasing repulsion of the Coulomb potential. (As a consequence the predicted "size" resonance of $\langle S_p \rangle$ versus A for a fixed energy would be very broad. By comparison, the neutron $3p$ size resonance near $A = 95$, observed, for example, by Camarda,[4] is relatively narrow.)

The mass region was included in a broader survey of (p,n) reactions by Schiffer and Lee[5] and by Elwyn, Marinov, and Schiffer.[6] Using thick targets of natural elements, they measured cross sections with ±10% relative and ±20% absolute uncertainties in 0.5-MeV steps from about 3 to 6 MeV (for our mass region). Their reduced (p,n)

Multipole moments of ^{154}Sm, ^{176}Yb, ^{232}Th, and ^{238}U from proton inelastic scattering

C. H. King,* J. E. Finck,† G. M. Crawley, J. A. Nolen, Jr., and R. M. Ronningen
Cyclotron Laboratory, Michigan State University, East Lansing, Michigan 48824
(Received 25 June 1979)

We have measured the inelastic scattering of 35 MeV protons from the nuclei ^{154}Sm, ^{176}Yb, ^{232}Th, and ^{238}U. Angular distributions were extracted for $J^\pi = 0^+$–8^+ members of ground state rotational bands. These data were analyzed using coupled channels calculations for scattering from a deformed optical potential. Searches were made on some of the parameters of this potential, including the deformation parameters β_2 and β_4. The multipole moments of the potential distribution were calculated from the parameter values and are compared to the results of Coulomb excitation, electron scattering, and inelastic, alpha-particle scattering studies. In general, these moments deduced in our investigation agree better with those from Coulomb excitation and electron scattering than with moments deduced from α-particle scattering. But we also find the moments from our study to be systematically smaller than those from Coulomb excitation.

[NUCLEAR REACTIONS ^{154}Sm(p,p'), ^{176}Yb(p,p'), ^{232}Th(p,p'), and ^{238}U(p,p'), $E_p = 35$ MeV; enriched targets, nuclear emulsion plates (7 keV FWHM) and position-sensitive proportional counter (15 keV FWHM), magnetic spectrograph; measured $\sigma(Ep', \theta)$; coupled channels calculations, rotational model; deduced optical model and deformation parameters, quadrupole and hexadecapole moments; comparisons to Coulomb excitation, (e,e') and (α,α'), comparisons to Hartree-Fock calculations.]

I. INTRODUCTION

The shape of a nucleus is one of its most fundamental properties, but the precise determination of the nuclear shape is still an outstanding problem. The most extensive and accurate data on nuclear deformations have come from Coulomb excitation measurements. However, in practice, the information which can be obtained from such measurements is incomplete. Because of the rapid decrease of excitation probabilities for the higher-order moments, the Coulomb excitation technique is essentially restricted to determinations of quadrupole (E2) and hexadecapole (E4) moments. Even the hexadecapole moment is often difficult to obtain precisely and is subject to ambiguities. (See, for example, Ref. 1 and references cited therein.) More importantly, Coulomb excitation is sensitive only to the charge distribution of a nucleus, and although information about higher charge moments might be obtained from higher momentum-transfer Coulomb measurements, such as high-energy electron scattering, information about the neutron distribution of a nucleus requires hadronic probes.

The standard technique for investigating nuclear shapes is the measurement of inelastic scattering cross sections. However, because the nuclear interaction is poorly understood and is much more complicated than the electromagnetic interaction, it is difficult to make model-independent determinations of nuclear shapes from such measurements. For simplicity it is usual to analyze the data in terms of a parametrized deformed optical model potential[2] (DOMP), which is a complex projectile-nucleus potential as in the normal optical model but with additional parameters describing the deformation of the nuclear surface. The parameters are then adjusted to fit both the elastic and inelastic scattering cross sections. The phenomenological nature of this model makes the deformation parameters (β_λ) determined by such an analysis rather uncertain and difficult to compare with Coulomb excitation results. Recently, Mackintosh[3] has pointed out that deformed optical model potentials which are derivable from a simple folding prescription (sometimes called the reformulated optical model[4]) have the property that their multipole moments are proportional to those of the underlying matter distribution. Thus, to the extent that the DOMP satisfies this property, the moments of the mass distribution can be determined in a model-independent way.

Most of the hadron scattering data on heavy nuclei have come from measurements using complex projectiles, principally the pioneering α-scattering measurements of Hendrie et al.[5] However, protons appear to have several possible advantages over composite projectiles as probes of the neutron distribution. The parametrized optical-model potentials for α-particles are known to possess many more ambiguities than those for protons making proton scattering a more suitable candidate for the moment analysis suggested by Mackintosh. In addition, the fact that the p–n interaction is stronger than the p–p and n–n interactions makes proton scattering more sensitive to the neutron distribution. Furthermore, the higher penetrability of protons in nuclear matter allows them to probe the nuclear interior, and the electron-scattering data of Cooper et al.[6] have given preliminary indications that for some deformed nuclei the deformations in the interior may be different from those at the surface. Finally, proton scattering should lend itself more readily to more fundamental analyses such as those using folding-model potentials.

Almost all proton scattering on heavy deformed nuclei has been measured at fairly low proton energies where the angular distributions are not sufficiently diffractive to be very sensitive to nuclear deformations. The purpose of the present study is to provide higher energy (p,p') data so that the possible advantages of proton scattering as a probe of nuclear deformations can be realistically assessed. We have chosen a proton bombarding energy of 35 MeV and the targets ^{154}Sm, ^{176}Yb, ^{232}Th, and ^{238}U, all of which have been studied by both Coulomb excitation and electron scattering. For the present we have chosen to analyze the data in the usual manner with a DOMP and will try to relate the results to those from the Coulomb measurements using the multipole moment

PHYSICAL REVIEW C VOLUME 20, NUMBER 6 DECEMBER 1979

Multinucleon transfer reactions induced by ^{18}O on ^{28}Si

M. C. Mermaz, A. Greiner, B. T. Kim, M. A. G. Fernandes, N. Lisbona, and E. Müller
Dph-N/BE, CEN Saclay, BP2, 91190 Gif-sur-Yvette, France

W. Chung and B. H. Wildenthal
Cyclotron Laboratory, Michigan State University, East Lansing, Michigan 48823
(Received 15 June 1979)

The experimental angular distributions of several multinucleon transfer reactions induced by ^{18}O on ^{28}Si have been measured and compared with distorted-wave reaction calculations. The shape and relative intensities of the data can be reproduced by theoretical calculations which seem to open the way for this type of study of structure of nuclei in the middle of the $2s$-$1d$ shell. On the other hand, we have not found it possible either to reproduce the shapes of the angular distributions with an optical potential derived from an elastic scattering analysis or to correctly calculate the absolute values of the cross sections. These difficulties which are similar to those encountered in other heavy-ion reaction studies will require extended improvements in the current formulations of the theory for the reaction processes.

[NUCLEAR REACTIONS $^{28}Si(^{18}O, ^{16}O)$, $^{28}Si(^{18}O, ^{20}Ne)$, $^{28}Si(^{18}O, ^{22}Ne)$, $^{28}Si(^{18}O, ^{15}N)$, and $^{28}Si(^{16}O, ^{15}O)$ $E_{^{18}O} = 56$ MeV—angular distribution measured between 5° and 35° laboratory angles—distorted wave reaction analysis; shell-model structure analysis.]

I. INTRODUCTION

Multinucleon transfer reactions induced by heavy ions have been used in various contexts to study aspects of nuclear structure such as four particle[1,2] and two particle[3,4] correlations. The reaction mechanism has been studied in detail for two-nucleon transfer and found to be quite complicated in that second order processes, such as core excitation preceding and/or following the transfer of nucleons, have to be taken into account.[5] In the vicinity of the Coulomb barrier, these multistep processes give rise to different shapes for the angular distributions depending upon the importance of the core excitation route which allows, in principle, detailed tests of the wave functions of the relevant nuclear states. This behavior has been widely tested in two-neutron and two-proton transfer reactions.[4,5] Their differential cross-sections are in fact very sensitive, not only to the values of the spectroscopic amplitudes involved, but also to their phases.

In both the simple and coupled channel distorted wave reaction calculations of heavy-ion transfer reactions, experience has shown that a principal difficulty is to find a potential which will reproduce simultaneously the elastic, the inelastic, and the transfer differential cross sections.[6] The disagreement between experimental data for transfer reactions and predictions based on potentials which reproduce the elastic scattering can be extremely large: Bell shaped angular distributions centered at a backward angle are obtained in the calculations while the experimental points display a forward peaked oscillatory pattern. This disagreement can be suppressed by decreasing arbitrarily the effective Coulomb barrier in the surface region. This can be effected by increasing either the radius of the charge distribution or the diffusivity of the real potential. The calculated angular distributions resulting from these adjustments are focused to forward angles. The improvement of the fit can also be pursued by using "surface transparent" potentials which have weak absorption at the nuclear surface,[7] i.e., potentials which have the radius and the diffusivity of the imaginary part smaller than those of the real part. A second difficulty with multinucleon transfer is the reproduction of absolute cross-section values. The so-called "unhappiness factors" ($N = \sigma_{exp}/\sigma_{theory}$) typically range between 10 and 100.

In spite of these difficulties it remains possible to extract spectroscopic information from these data, if a consistent empirical formulation of the reaction process yields shapes and apparent relative normalizations in agreement with observation. It appears that distorted wave Born approximation (DWBA) calculations, in cases where one step processes dominate, and coupled channel Born approximation (CCBA) calculations, where multistep processes are important, satisfy this requirement. The possibility of doing studies with two-nucleon transfer reactions has been confirmed for instance in the $1f$-$2p$ shell for Ni, Ge, and Mo

The two-step pickup-stripping process in the $^{24}Mg(p,p')^{24}Mg$ reaction at 40 MeV to some negative parity states in ^{24}Mg

B. Zwiegliński,* G. M. Crawley, and J. A. Nolen, Jr.
Cyclotron Laboratory and Department of Physics, Michigan State University, East Lansing, Michigan 48824
(Received 16 April 1979)

Remarkably similar bell-shaped angular distributions are observed in the $^{24}Mg(p,p')$ reaction at 40 MeV to some negative parity states in ^{24}Mg. Two-step (p,d,p') coupled channel calculations give a good account of these angular distributions.

[NUCLEAR REACTIONS $^{24}Mg(p,p')^{24}Mg$, $E=40$ MeV; measured $\sigma(E_p;\theta)$, $E_p=8.864$, 9.148, and 11.293 MeV; CRC (p,d,p') calculations, deduced reaction mechanism.]

The microscopic distorted-wave Born approximation (DWBA) theory of proton inelastic scattering treats the reactions as a one-step process mediated by the effective two-body force. Introduction of antisymmetrized DWBA codes and the derivation of the two-body force from the free nucleon-nucleon potentials were major recent improvements and have made inelastic proton scattering a useful spectroscopic tool. The DWBA gives a valid description of the scattering, provided that the coupling to the entrance channel is weak and that higher-order processes are not important. The higher-order processes associated with the collective degrees of freedom have been extensively studied in the past and gave valuable information on, e.g., nuclear deformation parameters. Another type of higher-order process, with which we are mostly interested in this paper, is associated with the single-particle degrees of freedom and involves consecutive transfer of a nucleon or nucleon cluster. Processes of this kind have been found important for many reactions,[1] including proton elastic scattering.[2] However, the occurrence of the pickup-stripping (p, d, p') process in (p, p') has not been conclusively demonstrated. The calculations of Ascuitto *et al.*[3] and more recent calculations of Amakawa *et al.*[4] have been compared with the data at a bombarding energy of about 10 MeV, an energy which is much too low to guarantee a pure direct mechanism. Hefter *et al.*[5] attempted to determine the contribution of the two-step (p, d, p') mechanism to the strongly collective 3^- states in ^{16}O and ^{40}Ca from the difference between the experimental and the DWBA cross sections calculated with large-basis random-phase approximation (RPA) wave functions. However, the theory predicted cross sections which were too large at backward angles, making it questionable whether the differences at forward angles could be due to the (p, d, p') process.

In our previous study[6] of the $^{24}Mg(p, p')^{24}Mg$ reaction at 40 MeV many transitions were fitted reasonably well by the one-step microscopic calculations. However, for the transitions to the 2^- 8.864 MeV and 1^- 9.148 MeV states remarkably similar bell-shaped angular distributions are observed which deviate strongly from the one-step DWBA predictions [see Fig. 1(a), dashed lines]. The antisymmetrized code DWBA 70 (Ref. 7), the two-body force of Bertsch *et al.*,[8] and the proton optical potentials of Table I were used in these calculations. It is the subject of the present work to demonstrate that the (p, d, p') process can explain the shapes and magnitudes of these angular distributions. As a spectroscopic application of the (p, d, p') process an attempt is made to determine the dominating single-particle components for these transitions.

The experiment was performed using 40 MeV protons from the MSU isochronous cyclotron. A 310 $\mu g/cm^2$ thick metallic foil enriched to 98.8% of ^{24}Mg was used as a target. Scattered particles were momentum analyzed with the Enge split-pole spectrograph and detected with a position-sensitive proportional counter in the spectrograph focal plane. Typical energy resolution was 16 keV.

The coupled-reaction-channels (CRC) code CHUCK[9] was used to interpret the data in terms of the two-step (p, d, p') process. The deuteron optical potential (Table I) found from the fits to the elastic scattering data[10] was used for the intermediate states. Bound-state wave functions were calculated with the separation energy method.

The low-lying negative parity states in the middle of the $2s1d$ shell can be formed by promoting a nucleon from the valence $2s1d$ to the $1f2p$ shell or from the filled $1p$ to the valence shell. The inset to Fig. 1 summarizes the experimental facts from the pickup reactions on ^{24}Mg (Refs. 12–15).

Mass and excited states of the nucleus ^{89}Mo

R. C. Pardo,* L. W. Robinson, W. Benenson, E. Kashy, and R. M. Ronningen
Cyclotron Laboratory, Michigan State University, East Lansing, Michigan 48824
(Received 4 June 1979)

The mass excess of ^{89}Mo has been measured using the ^{92}Mo(^{3}He,^{6}He) reaction at 70-MeV bombarding energy. The mass excess was determined to be -75.008 ± 0.015 MeV. The excited states observed are also reported.

[NUCLEAR REACTIONS ^{92}Mo(^{3}He, ^{6}He)^{89}Mo; $E = 70$ MeV, measured reaction Q values, deduced mass excess, excitation energies.]

The (^{3}He, ^{6}He) reaction has been used extensively for studying the properties of proton-rich nuclei, especially in the lighter mass region. Recently we have used it to measure the masses of a number of medium mass nuclei.[1] These measurements not only test the accuracy of mass relations in the proton-rich region but also provide important outposts for future β-decay mass determinations. In this communication we report the mass and excited states of the isotope ^{89}Mo.

The β^+ decay of ^{89}Mo was first reported by Butement and Qaim.[2] They reported an activity of 7 min half-life based on the observation of positrons with energies greater than 3.6 MeV. The β^+ endpoints observed were 4.05 and 4.95 MeV. No γ rays were observed in the decay. The results of our work show that the maximum β^+ decay energy available in the decay of ^{89}Mo is 4.59 MeV. Therefore, the 4.95-MeV activity observed could not have been ^{89}Mo. Much later, Hagenour *et al.*[3] attempted to study ^{89}Mo. Using three different targets, two projectiles, and seven energies they reported no activities which could be identified as ^{89}Mo. Systematics in this region predict a half-life of 1–2 minutes for ^{89}Mo. Based on these considerations, we doubt that the activity observed in Ref. 2 was really ^{89}Mo.

The Michigan State University cyclotron provided 70-MeV ^{3}He beams with intensities of approximately 700 nA on target. Reaction products were identified in the focal plane of an Enge split-pole spectrograph with a two wire, charge-division proportional counter in a manner described in Ref. 1. The resolution obtained was approximately 60 keV. A target of 260 μg/cm^2 thickness was produced by electron sputtering 98.3% enriched ^{92}Mo onto a 20 μg/cm^2 carbon foil reinforced by 2 μg/cm^2 Formvar. The principal calibration reaction chosen was ^{26}Mg(^{3}He, ^{6}He). The ^{26}Mg target used was a 251 μg/cm^2 self-supporting foil. Target thickness was determined by α-gauge measurements using 8.784-MeV α particles from ^{228}Th decay products.

Calibration of the spectrograph was accomplished in a two stage manner. First, the ^{27}Al(^{3}He, α) reaction was used to calibrate the detector in mm/channel. The ^{26}Mg(^{3}He, ^{6}He) reaction then served as the reference reaction. This reaction was chosen because its Q value of -13.407 ± 0.002 MeV allows the entire experiment to be performed at the same spectrograph field setting. The mass excesses used for the relevant nuclei involved in the calibration are those of Wapstra and Bos.[4]

The results reported here are based on data taken at 7° and 10° laboratory angles. In an effort

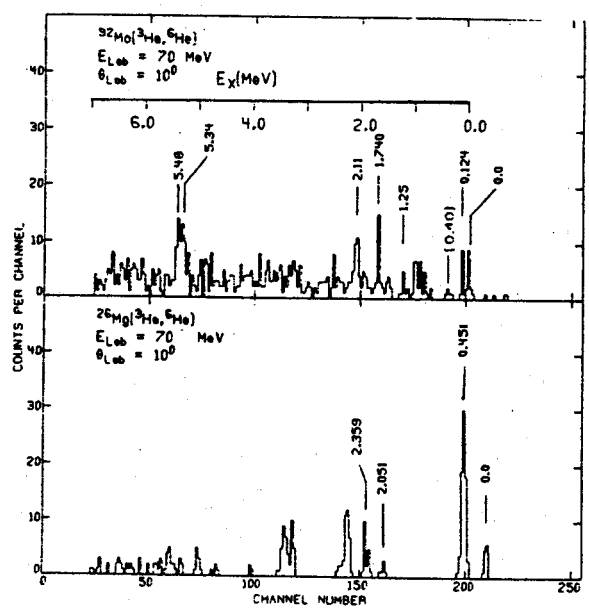

FIG. 1. Spectrum of all events from the ^{92}Mo(^{3}He, ^{6}He) reaction ($Q_{total} = 37\,000$ μC) and the calibration reaction ^{26}Mg(^{3}He, ^{6}He). Both spectra were taken at the same spectrograph field strength.

$^{14}N(p,p')^{14}N$ reaction between 25 and 40 MeV and the tensor part of the effective interaction

S. H. Fox*
Cyclotron Laboratory and Physics Department, Michigan State University, East Lansing, Michigan 48824

Sam M. Austin
Cyclotron Laboratory and Physics Department, Michigan State University, East Lansing, Michigan 48824 and Sektion Physik, Universität München, D-8046 Garching, West Germany

(Received 30 August 1979)

Differential cross sections for the scattering of protons from ^{14}N, leaving this nucleus in its ground, 2.31- or 3.95-MeV states, were measured at bombarding energies of 29.8, 36.6, and 40.0 MeV. In addition, cross sections for the next ten excited states with $E_x < 8.7$ MeV were obtained at 29.8 MeV. Emphasis was placed on obtaining reliable results for the transition to the weakly excited $J^\pi = 0^+$, $T = 1$ state at 2.31 MeV, which is unusually favorable for studies of the tensor part of the effective interaction. The present data for the 2.31-MeV state, together with results from the literature at $E_p = 24.8$ MeV, were analyzed using a microscopic model distorted-wave approximation; contributions from the knock-on exchange amplitude and from central, tensor, and spin-orbit two-body forces were included. The fits obtained were satisfactory at 24.8 and 29.8 MeV, but failed to reproduce a peak in the cross section which appeared near 80° at the higher bombarding energies. Strengths of the tensor force were extracted and were found to be 20–75% larger than estimates based on the one-pion-exchange potential. Available evidence on the strength of the tensor force is summarized. Of the other observed states, those whose structure is dominated by 1p-shell orbitals [at 3.95 MeV (1^+, $T = 0$) and at 7.03 MeV (2^+, $T = 0$)] were compared with microscopic distorted-wave approximation calculations using an empirically derived central force. Cross section enhancement factors were calculated in an effective charge approximation. The resulting cross sections have roughly the correct magnitude, but the shapes are only qualitatively correct. A systematic optical model analysis was carried out to provide optical model parameters for use in the distorted-wave approximation calculations. The rate of change of the real potential with bombarding energy was found to be $dV_R/dE_p = -0.50$.

[NUCLEAR REACTIONS $^{14}N(p,p')$, $E = 29.8$, 36.6, 40.0 MeV; measured $\sigma(\theta)$. Deduced optical model parameters. Microscopic distorted-wave analysis, deduced tensor effective interaction.]

I. INTRODUCTION

A number of studies of the role played by the tensor force in nuclear reactions and structure have involved the mass-14 system. The tensor force first became associated with this system through efforts to explain the anomalous Gamow-Teller β decay of ^{14}C to ^{14}N(g.s.).[1-3] Although allowed by the selection rules ($(J^\pi = 0^+, T = 1) \rightarrow (1^+, 0)$), this decay is found experimentally[4] to be strongly suppressed, having a log ft of 9.02. For a nuclear structure model with only 1p–shell orbitals, it has been shown[3,5,6] that no central-plus-spin-orbit two body interaction can account for this inhibition, but that it can be explained[1-3] by including a tensor force.

One also expects that the two body effective interaction V_{eff} used in microscopic theories of inelastic scattering and charge exchange reactions will have a tensor component. While this component is usually overwhelmed by the stronger central parts of the interaction,[7] this should not be the case for the $^{14}N(p,p')^{14}N$ (2.31 MeV) reaction we consider here or for its isospin analogs such as the $^{14}C(p,n)^{14}N$ (g.s.) reaction. A transition between states with these quantum numbers $(0^+, 1 \rightarrow 1^+, 0)$ would normally be dominated by the central force part of the transition amplitude. However, since the angular momentum transfer $L = 0$ part of this central-force amplitude, is closely proportional to the matrix element for allowed β decay between these states,[8-10] it will be suppressed for the same reason the β decay is suppressed and the tensor force should be observable. The extraction of the tensor force strength should be facilitated by the fact that the remaining $L = 2$ central force contribution will have a relatively broad shape, while the tensor force contribution will be strongly forward peaked.

There have been a number of studies of this $(1^+, 0) \leftrightarrow (0^+, 1)$ transition: $^{14}C(p,n)^{14}N$ (g.s.),[8,9,11,12] $^{14}N(p,n)^{14}O$ (g.s.),[12,13] $^{14}N(p,p')^{14}N$ (2.31 MeV),[14-17] and $^{14}N(n,n')^{14}N$ (2.31 MeV).[18] It was usually found[11-17] that including a tensor force substantially improved the description of the data, and the extracted tensor force strengths were roughly consistent with the one-pion-exchange potential (OPEP). However, the fits obtained were often of poor quality. In addition, much of the work was at energies below 20 MeV so that one could not, on a priori grounds, exclude contributions from compound nuclear processes[15] for these light nuclei. In other cases, the angular range and/or accuracy of the data was not sufficient to stringently test the theoretical model.

The present work was undertaken to obtain accurate data on the $^{14}N(p,p')^{14}N$ reaction over an extended energy and angular range. The main results reported are angular distributions for the 0.0, 2.31 and 3.95 MeV states of ^{14}N at bombarding energies of 29.8, 36.6 and 40.0 MeV. In addition, angular distributions for the next ten excited states with $E_x < 8.7$ MeV were obtained at 29.8 MeV. The experimental method and results are described in Sections II and III. Optical model fits to the elastic scattering data are described in Section IV and a brief outline of the distorted wave approximation (DWA) is given in Section V. Microscopic DWA calculations including contributions from the knock-on exchange amplitudes and from central, tensor and spin-orbit forces were carried out for those states which are well described by 1p–shell wave functions. The emphasis was on extraction of the strength of the tensor force from the data for the 2.31 MeV state. These calculations are discussed in Section VI. Finally, in Section VII, the results

Inelastic scattering of ^{6}Li from ^{58}Ni at 71 MeV

C. Williamson,* A. Galonsky, R. Huffman,† and R. Markham‡
Cyclotron Laboratory, Michigan State University, East Lansing, Michigan 48824
(Received 31 October 1979)

Nine excited states of ^{58}Ni were studied via the ^{58}Ni(^{6}Li,^{6}Li) reaction at 71.2 MeV. Two methods were employed to analyze the data. They were the distorted wave Born approximation, and the method of coupled channels. A comparison of their predictions and the information they provide about the nuclear deformation lengths is presented. In agreement with the Austern-Blair model for strongly absorbed particles, all five parameter sets produced equally good fits to the inelastic data.

[NUCLEAR REACTIONS ^{58}Ni(^{6}Li,^{6}Li') for ^{58}Ni* energies E^{*} = 1.45, 2.46, 2.78, 3.04, 3.26, 3.62, 3.90, 4.48, and 4.75 MeV. Angular distributions measured, deformation lengths extracted.]

I. INTRODUCTION

Elastic[1-5] and inelastic[3,4] scattering of ^{6}Li by medium weight nuclei have been studied recently, but none of the studies has investigated inelastic transitions in ^{58}Ni with projectile energies above 34 MeV. In the present work nine inelastic transitions were observed in ^{58}Ni at 71 MeV. Each transition was treated as a one-phonon collective transition in the DWBA using complex coupling. Since the deformations of separate portions of the interaction potential (real, imaginary, Coulomb) need not necessarily be equal, the calculations were performed twice with each set of optical model (OM) parameters that fits the elastic scattering data.[5] These parameters are listed in Table I. In one set of calculations, the deformations were held equal, and in the other set of calculations the deformation lengths were held equal.

Preliminary coupled-channels calculations were also performed for the lowest energy, $0^{+}-2^{+}-4^{+}$, vibrational band which coupled the ground state and first two excited states. Investigations into multiple-plus-direct with admixtures of one-and two-phonon transitions for the first 4^{+} state at 2.45 MeV were performed with α-particle scattering as early as 1962 by Buck[6] and as recently as 1972 by Horen et al.[7] The studies were prompted by the fact that this state does not follow the Blair phase rule. According to this rule, angular distributions corresponding to even values of angular momentum transfer L should be out of phase with angular distributions corresponding to odd L transfer. Also, angular distributions with odd L should be in phase with the elastic distributions.

For the ^{90}Zr + ^{6}Li reaction at 34 MeV[3] and 75 MeV,[8] sizable differences have been noted between extracted deformation lengths and previously reported values. Surprise at these observations was one motivation in performing this investigation.

Table I. Optical model parameter sets which give the best fits to the elastic scattering data of Huffman et al.[5]

V	r_R	a_R	W	r_I	a_I
60	1.43	.84	17.6	1.78	.78
110	1.26	.86	18.0	1.77	.78
160	1.17	.87	18.8	1.76	.78
225	1.07	.89	19.9	1.74	.78
296	1.01	.89	21.5	1.72	.78

II. EXPERIMENTAL PROCEDURES

The MSU sector-focused cyclotron was used to produce an extracted beam of 200-300 nA of $^{6}Li^{+++}$ ions. An arc-like ion source[9] produced the beam through the sputtering action of Ne on LiF pellets, enriched in ^{6}Li. Electrodes of tantalum (source life, approximately three hours) were used, but hafnium was briefly employed in an attempt to increase source life.[10] (Hafnium did increase source lifetime by approximately a factor of two, but on-target current was reduced by a factor of approximately four.) Two analyzing magnets and several quadrupole focusing magnets were used to give a rectangular beam spot of approximately 2 mm x 4 mm on a foil target of 1.02 mg/cm^{2}, 99% enriched ^{58}Ni. On-target beam intensity of 10-50 nA at 71.2 MeV was monitored by stopping the beam in a Faraday cup and sending the current to an Ortec charge digitizer for charge measurements.

A detector with two resistive-wire, position-sensitive proportional counters in sequence backed by a scintillator, placed in the focal plane of an Enge split-pole spectrograph was used to gather the data. Two-dimensional gating techniques (ΔE vs TOF (time-of-flight), ΔE vs position, TOF vs position, and light vs position) were used for multiple identification of the scattered lithium ions. A PDP-11/45 on-line computer was used for gating, display, and collection of data.

The low beam intensity restricted the range over which it was possible to gather data to lab angles less than approximately 45°. A FWHM ~ 90 keV made it possible to resolve nine inelastic states. Typical spectra are displayed in Figure 1. For angles below 18°, the elastic peak was not recorded (see upper spectrum of Figure 1) in order to decrease dead-time in the detector. At the other angles, where the elastic peak was included in the spectra, we could obtain a check on the absolute values by comparison to the elastic-scattering data of Huffman et al.[5] at 74 MeV. To account for the 3-MeV difference, the OM parameter set (Table I) with V = 160 MeV was used to calculate the elastic scattering at 71 MeV. At some of the angles beyond 30°, where the runs were long, there were significant errors in our measurement of the elastic cross section. Therefore, we normalized our data by comparison of our elastic cross sections to those computed from

Transverse electromagnetic form factor in ^{12}C

D. Cha

Department of Physics and Cyclotron Laboratory, Michigan State University, East Lansing, Michigan 48824

(Received 16 July 1979)

We calculate the contribution from the convection current to the recently measured transverse form factor of the ^{12}C 2^+ level at 4.44 MeV. The convection current dominates for small momentum transfer and is determined by the $B(E2)$. In this region, theory agrees with experiment. At intermediate momentum transfer, agreement with experiment is only possible assuming a coherent sum of the convection current and magnetization density contributions.

[NUCLEAR STRUCTURE ^{12}C, $E=4.44$ MeV; calculated F_T^2.]

In a recent paper,[1] Flanz *et al.* measured the transverse electromagnetic form factor of ^{12}C 2^+ levels at 4.44 MeV ($T=0$) and at 16.1 MeV ($T=1$). Using the intermediate coupling shell model of Cohen and Kurath, they claimed strong discrepancy between theory and experiment for the form factor of the isoscalar state. The Cohen-Kurath model lacks a convection current, which dominates the transverse form factor at low momentum transfer.[2] In this note, we evaluate the convection current and find that it alone accounts for the low momentum transfer data. This is in accord with an analysis of earlier measurements[3] by Radomski,[4] who found consistency between experiment and a cranked rotor model. At intermediate momentum transfer, a coherent sum of contributions from the convection current and the magnetization densities is required.

We follow the notation of Flanz *et al.*, and write the transverse form factor as

$$F_T(q)^2=\frac{4\pi}{Z^2}\frac{1}{2J_i+1}\sum_{J=1}^{\infty}\{|\langle J_f\|\hat{T}^{el}_J(q)\|J_i\rangle|^2+|\langle J_f\|T^{mag}_J(q)\|J_i\rangle|^2\}. \quad (1)$$

The electric multipole $\hat{T}^{el}_{JM}(q)$ is given by[2]

$$\hat{T}^{el}_{JM}(q)=\frac{1}{[J(J+1)]^{1/2}}\frac{1}{q}\int[(\vec{\nabla}\times\vec{L}j_J(qr)Y_{JM}(\Omega))\cdot\vec{j}_N(\vec{r})+q^2(\vec{L}j_J(qr)Y_{JM}(\Omega))\cdot\vec{\mu}_N(\vec{r})]d^3r, \quad (2)$$

where $\vec{j}_N(\vec{r})$ and $\vec{\mu}_N(\vec{r})$ are the convection current and magnetization densities in the nucleus and $\vec{L}=-i\vec{r}\times\vec{\nabla}$ is the orbital angular momentum. The magnetic multipole does not contribute to $\Delta J^\pi=2^+$ transitions. Blatt and Weisskopf[5] simplify the integral for the convection current by integration by parts,

$$\int(\vec{\nabla}\times\vec{L}j_J(qr)Y_{JM}(\Omega))\cdot\vec{j}_N(\vec{r})d^3r=-\int j_J(qr)Y_{JM}(\Omega)L\cdot(\vec{\nabla}\times\vec{j}_N(\vec{r}))d^3r, \quad (3)$$

and use of the vector identity

$$\vec{L}\cdot(\vec{\nabla}\times\vec{j}_N)=-i[(\vec{r}\cdot\vec{\nabla}+2)(\nabla\cdot\vec{j}_N)-\vec{\nabla}^2(\vec{r}\cdot\vec{j}_N)]. \quad (4)$$

Current conservation allows the replacement of $\vec{\nabla}\cdot\vec{j}_N$ in the first term by $i(E_f-E_i)\hat{\rho}_N$. The second term vanishes in the rigid rotor approximation, since then $\vec{j}_N$ is perpendicular to $\vec{r}$. It also vanishes in the long wavelength limit, allowing the transverse form factor to be expressed completely in terms of the charge density operator $\hat{\rho}_N$. In either case we find that the electric multipole becomes

$$\hat{T}^{con}_{JM}(q)=-\frac{1}{[J(J+1)]^{1/2}}\frac{E_f-E_i}{q}\times\int j_J(qr)Y_{JM}(\Omega)\left(r\frac{\partial}{\partial r}+2\right)\hat{\rho}\,d^3r=\frac{1}{[J(J+1)]^{1/2}}\frac{E_f-E_i}{q}\int\frac{d}{dr}(rj_J(qr))Y_{JM}(\Omega)\hat{\rho}\,d^3r. \quad (5)$$

We now evaluate the matrix element Eq. (5) using the macroscopic model

$$\langle 2^+\|\hat{\rho}\|0^+\rangle=\beta R\frac{d\rho_0(r)}{dr}Y_{20}. \quad (6)$$

The transverse form factor is then given by

$$F_T(q)^2=\frac{4\pi}{Z^2}|\langle 2^+\|\hat{T}^{con}_2(q)\|0^+\rangle|^2=\frac{2\pi}{3}\frac{1}{Z^2}\left(\frac{E_f-E_i}{q}\right)^2(\beta R)^2\times\left|\int\left[\frac{d}{dr}(rj_2(qr)\right]\frac{d\rho_0(r)}{dr}r^2dr\right|^2. \quad (7)$$

To compare with the experiment, we use a

Relative importance of neutron and proton components of nuclear transitions and comparative π^-/π^+ inelastic scattering

B. A. Brown
Nuclear Physics Laboratory, University of Oxford, Oxford OX1 3RH, England

B. H. Wildenthal
Nuclear Physics Laboratory, University of Oxford, Oxford OX1 3RH, England
and Cyclotron Laboratory, Michigan State University, East Lansing, Michigan 48824

(Received 14 September 1979)

Shell-model calculations for ^{18}O and ^{26}Mg yield predictions of strong state dependence of the isovector component of nuclear transition strengths, with results for ^{18}O being consistent with recent measurements of π^-/π^+ inelastic scattering ratios.

[NUCLEAR STRUCTURE ^{18}O, ^{26}Mg; calculated neutron and proton components of inelastic scattering excitations; estimates of π^-/π^+ cross section ratios; shell model.]

For a complete understanding of nuclear structure it is necessary to be able to distinguish between the neutron and proton components of nuclear transitions. This problem has been addressed with conventional nuclear probes by comparing the reduced electromagnetic strength of a transition in a stable ($N > Z$) nucleus to the strength of the corresponding transition in the analog ($Z > N$) nucleus[1,2] or, alternatively, to the reduced strengths of the same transition in the ($N > Z$) nucleus as induced by hadronic probes such as protons or alphas.[3] The first of these approaches is complicated[1] by the necessity of dealing with the (often significant) differences[4] in the radial wave functions of the protons and neutrons in the two different nuclear systems. The second approach faces the problem of quantitatively relating the reduced strengths of a transition induced by completely different types of probes.

The new "meson factories" offer a fresh alternative approach to this problem via the measurement of the relative cross sections for excitation of a given nuclear level by the inelastic scattering of π^+ and π^- projectiles. The sensitivity of this measurement to the differences in the neutron and proton components of the transition comes from the fact that the resonant cross sections for the interactions of π^+ with protons and π^- with neutrons are about nine times larger than for the corresponding interactions of π^+ with neutrons and π^- with protons. Experimental results of studies on ^{18}O which employ this technique have recently been published.[5,6]

We present here some shell-model predictions for the isoscalar and isovector, or in other terms the neutron and proton, components of nuclear transitions in ^{18}O and ^{26}Mg. These shell-model predictions are used, together with the simplest possible assumptions about the π-nucleus reaction mechanism, to predict the results of π^-/π^+ inelastic scattering cross section ratios. The results for ^{18}O seem consistent with existing data and suggest that measurement of additional transitions in this system should prove very interesting. The results for ^{26}Mg explain the anomaly of the phase of the isovector term of the 0_1^+-2_1^+ transition noted in Ref. 1 and predict a striking difference between the relative neutron-proton structures of the 0_1^+-2_1^+ and 0_1^+-2_2^+ transitions.

The shell-model wave functions employed in the present analysis are obtained from calculations in which the space of basis vectors is generated either by the $0p_{1/2}$, $1s_{1/2}$, and $0d_{5/2}$ single-nucleon orbits[7] (a "^{12}C-core model") or by the $0d_{5/2}$, $1s_{1/2}$, and $0d_{3/2}$ orbits[8] (an "^{16}O-core model"). For $A = 18$, the ^{16}O-core model provides only a schematic accounting of the observed level structure. Accordingly, while such results are presented for ^{18}O, attention is principally focused upon the results of the ^{12}C-core model for this system. For ^{26}Mg, the ^{16}O-core model provides the appropriate degrees of freedom.

Our procedure is to condense the information contained in the nuclear wave functions which is relevant to a transition of angular momentum and isospin rank ΔJ and ΔT into the one-body-transition densities

$$D^{N;JT,J'T'}_{\Delta J,\Delta T}(j,j') = \frac{\langle \psi^{NJT} \| (a_j^+ \otimes \tilde{a}_{j'})_{\Delta J,\Delta T} \| \psi^{NJ'T'} \rangle}{(2\Delta J+1)^{1/2}(2\Delta T+1)^{1/2}}, \quad (1)$$

Neutron angular and energy distributions from 710-MeV alphas stopping in water, carbon, steel, and lead, and 640-MeV alphas stopping in lead

R. A. Cecil, B. D. Anderson, A. R. Baldwin, and R. Madey
Department of Physics, Kent State University, Kent, Ohio 44242

A. Galonsky, P. Miller, and L. Young*
Cyclotron Laboratory, Michigan State University, East Lansing, Michigan 48824

F. M. Waterman†
Department of Radiology, University of Chicago, Chicago, Illinois 60637
(Received 22 October 1979)

We measured neutron angular and energy distributions from 710-MeV alphas stopping in targets of water, carbon, steel, and lead for neutron energies from 3 MeV to above 300 MeV. We also measured neutron spectra from 640-MeV alphas stopping in lead. These spectra are similar to the 710-MeV spectra but are reduced in magnitude by about 20 percent. The angular distributions are forward peaked and have a broad bump at about 120 MeV in the 0- and 6-degree spectra. The 710-MeV integrated yields above 10 MeV are about 0.5 neutron per incident alpha, independent of the target. The measured spectra from the water target are consistent with the calculations of an intranuclear cascade model at the forward angles, but are larger than the calculations at the backward angles.

[NUCLEAR REACTIONS H_2O, C, steel, Pb(α,xn), E=710 MeV; Pb(α,xn), E =640 MeV. Measured unidirectional spectra and yields from thick targets. Deduced total integrated neutron yields above 10 MeV. Compared spectra with intranuclear-cascade model.]

I. INTRODUCTION

We measured unidirectional neutron spectra above 3 MeV at angles ranging from 0 to 150 deg produced by 710-MeV alpha particles stopping in targets of carbon, water, steel, and lead; in addition, we report some measurements of neutron spectra produced by 640-MeV alphas stopping in lead. These measurements were made at the Space Radiation Effects Laboratory in Newport News, Virginia. They were motivated by the need for data to design shielding for the superconducting heavy-ion accelerator at Michigan State University. These data for the light targets are of interest also for estimating neutron doses produced by nuclear interactions during irradiation of cancerous tumors with alpha beams. The measured spectra from the water target are compared with those calculated from an intranuclear-cascade model.[1]

II. EXPERIMENTAL PROCEDURE

The energy of a neutron produced in the target was measured by the time-of-flight (TOF) technique. We measured the time difference between the detection of an alpha particle in a beam telescope and the detection of a neutron in one of several counters located one to five m away from the target. The neutron energy was then calculated from the TOF of the neutron measured relative to the observed prompt gamma peak. Absolute neutron yields were determined from the number of incident alphas counted in the beam telescope and from the detection efficiency for each neutron counter as calculated with the computer code of Cecil *et al.*[2]

A. Experimental arrangement

Figure 1 shows the experimental arrangement and indicates a typical placement of five neutron counters. As many as six counters were used simultaneously during the experimental run. A 710-MeV alpha beam was extracted from the cyclotron and transported to the experimental area in an evacuated beam line. During one experimental run a copper degrader was used to reduce the 710-MeV beam to 640 MeV. The external alpha beam passed through a beam telescope consisting of two 7.6 cm by 7.6 cm by 0.79 mm thick NE-102 plastic scintillators shown as $S1$ and $S2$ in Fig. 1. Signals from $S1$ and $S2$ were used in a coincidence circuit to count the absolute number of beam particles incident on the target. The duration of the data-taking runs varied from about 1 to 4 h with a typical flux of 5×10^4 alphas per second incident on the target. After traversing

Inelastic scattering $E4$ transition probabilities in the $0d$, $1s$ shell

B. A. Brown
Nuclear Physics Laboratory, Oxford University, Oxford OX1 3RH, England

W. Chung
Cyclotron Laboratory, Michigan State University, East Lansing, Michigan 48824

B. H. Wildenthal
Nuclear Physics Laboratory, Oxford University, Oxford OX1 3RH, England
and Cyclotron Laboratory, Michigan State University, East Lansing, Michigan 48824*
(Received 25 January 1980)

Theoretical $E4$ transition matrix elements calculated in the full $d_{5/2}$-$s_{1/2}$-$d_{3/2}$ shell-model space are presented for excitations of some ground states of stable nuclei for $18 \leq A \leq 38$. These matrix elements have been used to calculate inelastic transition probabilities for electromagnetic and hadronic probes. Available data on the relative magnitudes and energy distributions of $E4$ excitation strengths are found to be well reproduced theoretically thereby. Based on several experimentally measured transition strengths, the empirical isoscalar $E4$ effective charge is found to be $e_p + e_n = (2.0 \pm 0.2)e$. This is similar in magnitude to the analogous isoscalar $E2$ effective charge, but is much larger than existing theoretical estimates.

[NUCLEAR STRUCTURE ^{18}O, ^{19}F, ^{20}Ne, ^{22}Ne, ^{24}Mg, ^{25}Mg, ^{26}Mg, ^{28}Si, ^{30}Si, ^{32}S, ^{34}S, ^{36}Ar, ^{38}Ar; calculations for the strengths of $E4$ inelastic scattering transitions and their proton and neutron components; complete $0d_{5/2}$-$1s_{5/2}$-$0d_{3/2}$ shell-model wave functions; Chung-Wildenthal Hamiltonians.]

I. INTRODUCTION

In this paper we present calculations for the strengths of $\Delta J^\pi = 4^+(E4)$ excitations of ground states in the region $18 \leq A \leq 38$. The one-body transition density matrix elements for these excitations were calculated from the $d_{5/2}$-$s_{1/2}$-$d_{3/2}$ shell-model wave functions of Chung and Wildenthal.[1,2] These transition densities were then used to calculate matrix elements for electromagnetic excitation of these transitions and for the relative strengths of these same transitions as they are excited by various hadronic probes. The present calculations systematically employ harmonic-oscillator single-particle wave functions. The effects of using different (e.g., Hartree-Fock) radial dependences for the single-particle states were examined and found to be significant, but no alternative clearly preferable to harmonic-oscillator dependence was determined.

Our present study focuses on three aspects of $E4$ phenomena. The first issue we address presumes reasonably good theoretical-experimental agreement between *relative* values of several large measured transition strengths. In such a context it is meaningful to speak of the "effective charges" appropriate to the model space which serve to produce agreement between calculation and experiment in the absolute as well as relative sense. By comparing values from the extant body of measured $E4$ rates to our calculated values we are able to extract a value of the isoscalar $E4$ effective charge for the sd-shell space of $e_p + e_n = (2.0 \pm 0.2)e$.

We then proceed to deal with the general questions of what type of $E4$ phenomena are predicted by the Chung-Wildenthal wave functions and how well these accord with experimental facts. There are several aspects to be considered, such as the dependence of the aggregate $E4$ strength on the A value, the distribution of strength within a given nucleus as a function of excitation energy, and the A dependence of this distribution.

Lastly, we consider the individual neutron and proton components of the transitions in the $T \neq 0$ nuclei. From the values of these components the relative strengths by which a given state is excited by various hadronic probes, as well as electronmagnetically, can be predicted. We consider in particular, alphas, protons, and pions.

In Sec. II the calculation of the shell-model transition-density matrix elements is described as well as their combination with the single-particle matrix elements (which incorporate the radial wave function dependence) to obtain the theoretical $B(E4)$ values. In Sec. III these values are compared with the strong experimental $B(E4)$ values to obtain $E4$ effective charges. In addition, the

2.E

Nuclear Physics A329 (1979) 429–449

THE REACTIVE TWO-BODY PART OF THE PION-NUCLEUS OPTICAL POTENTIAL

J. CHAI† and D. O. RISKA

Department of Physics and Heavy Ion Laboratory, Michigan State University, East Lansing, Michigan 48824

Received 23 April 1979

Abstract: We calculate the reactive component of the two-body contribution to the pion-nucleus optical potential from a two-nucleon pion absorption mechanism that predicts the total cross section and angular distributions for $\pi^+ d \to pp$ very well. At threshold the calculated absorptive parts explain most of the values obtained from pionic atom level widths, whereas the dispersive parts, which are very sensitive to wave function correlations are considerably more attractive than what the conventional phenomenological parameters would suggest.

1. Introduction

Recently several papers have been published on the problem of deriving the two-body parts of the pion-nucleus optical potential, i.e. the parameters B_0 and C_0 in the potential expression

$$2\omega U_{\text{opt}}^{(2)} = -4\pi[B_0\rho^2 - \nabla C_0 \cdot \rho^2 \nabla], \tag{1}$$

(ω = pion energy, ρ = nuclear density) from basic two-nucleon absorption mechanisms. The threshold value for B_0 has been calculated by Hachenberg and Pirner [1]) and Bertsch and Riska [2]), and the absorptive value Im B_0 above threshold by Chai and Riska [3]). The P-wave parameter C_0 has been calculated by Miller [4]), Ko and Riska [5]) and very recently by Oset, Weise and Brockman [6]). Very related work on P-wave absorption has also been carried out by Rockmore, Kanter and Goode [7]), although without presentation of explicit results for C_0.

In all of these works the input to the calculation is a two-nucleon pion absorption mechanism in which either a pion or a ρ-meson is rescattered from one nucleon to another, as illustrated in figs. 1a and 1b. That such models actually can explain not only the total cross section but the angular distributions as well for the fundamental test reaction $pp \to d\pi^+$ has been recently demonstrated [8,9]).

The input amplitudes in fig. 1 may be decomposed into parts related to S-wave and P-waves in the πN system. The former is responsible for all of B_0 and gives but a small contribution to C_0, whereas the latter contributes the dominant part of C_0. This separation can however be complicated by effects of transformation of variables

† Supported by the National Science Foundation.

1.B: 2.B

Nuclear Physics A 338 (1980) 349–376

ON THE REACTIONS $\bar{p}p \leftrightarrow d\pi^+$

J. CHAI*† and D. O. RISKA

Department of Physics
and
Heavy Ion Laboratory, Michigan State University, East Lansing, Michigan 48824, USA

Received 9 October 1979

Abstract: The total cross section for $\pi^+ d \to pp$ and the angular distribution and asymmetry parameters for the inverse reaction $\bar{p}p \to \pi^+ d$ have been calculated with different models for the pion absorption (and production) operator and several sets of nuclear wave functions. The absorption operator includes both single-nucleon and two-nucleon operators. Fair agreement can be achieved with all empirical parameters at low energies, but significant discrepancies occur at high energies. The results are very sensitive to the model for the nucleon-nucleon interaction used to generate the wave functions.

1. Introduction

The ideal reactions for testing models for pion production and absorption mechanisms in nuclei are the two-nucleon pion-production reaction $pp \to d\pi^+$ and its inverse. Consequently considerable experimental and theoretical interest in these reactions has been expressed in the recent literature. The simplest model that can lead to an acceptable prediction for their total cross sections is that based on pion-nucleon rescattering, illustrated in fig. 1a [ref. [1]]. If the vertices of the intermediate pion are assumed to have a spatial extent of relatively long range that can be described by a form factor with a mass scale of 600–800 MeV/c^2, the otherwise far too large calculated cross section can be brought down to reasonable values [2,3]). An alternative model, which involves ρ-meson in addition to pion rescattering as illustrated in fig. 1b, permits usage of vertex form factors associated with far shorter range [4,5]). This second model which puts less reliance on phenomenological form factors, apart from being *a priori* more appealing, actually leads to considerably better predictions for the total cross sections at low energies. As it has also been shown that these mechanisms can explain most of the empirical absorption rates in nuclei [6–8]) it becomes interesting to study them in more detail in the fundamental two-nucleon reactions.

Going beyond the lowest-order perturbation theory approach based on the diagrams in fig. 1, Niskanen [9]) has recently calculated the angular distribution and

* Supported by the National Science Foundation.
† Present address: Physics Department, Old Dominion University, Norfolk, VA 23508, USA.

LETTERE AL NUOVO CIMENTO VOL. 26, N. 5 29 Settembre 1979

The (p, t_0) Angular Distribution with Deep Minima and the Geometrical Aspect of the DWBA Calculation.

Y. IWASAKI, E. KASHY and R. G. MARKHAM (*)

Cyclotron Laboratory, Michigan State University - East Lansing, Michigan 48824, *U.S.A.*

(ricevuto il 16 Luglio 1979)

The experimental angular distribution for the ground-state transition in the (p, t) reaction on a spherical, doubly even target nucleus has unique features: 1) it is a rapidly changing function of the reaction angle, having sharp peaks and deep minima, and 2) it is a very slowly varying functional of the target mass number and charge at a fixed incident energy. These features suggest that the experimental (p, t_0) angular distribution reflects geometrical properties of the nucleus such as nuclear radius or surface diffuseness. If this is really the case, geometrical properties of the nucleus are important in the calculation of the (p, t_0) angular distribution. In the distorted-wave Born approximation (DWBA) theory of the (p, t) or (t, p) reaction, the geometrical properties of the nucleus are expressed by the geometry of the proton and triton optical potentials and the neutron-binding potential. The present note calls attention to the geometrical aspect of the DWBA calculation of the (p, t_0) angular distribution, criticizes the prevalent neglect of it that amounts to the common practice of using standard (average)-fixed-geometry optical potentials, and demonstrates the importance of the geometrical aspect by showing that the target-nucleus dependence of the (p, t_0) angular distribution is mostly a simple geometrical effect.

Almost all analyses of (p, t) reaction data were performed by the zero-range DWBA theory. The practice usually found in the literature is to try some several sets of optical potentials determined by proton and triton elastic-scattering data or derived from some sources and to choose a set that gives a best overall fit to the (p, t) data. This procedure, which is generally unable to give an excellent fit to the experimental (p, t_0) angular distribution, originates from the common belief that the optical potentials to be used in the DWBA calculation of a transfer reaction can be and should be determined by the differential elastic-scattering cross-sections. There are well-known ambiguities, however, in the determination of the optical potential by a best fit to the differential elastic-scattering cross-sections [1]. One of the ambiguities is the continuous ambiguity concerning the well-depth V and the radius parameter r_0 of the real central well. Potentials having different sets of values of V and r_0 give almost equally good fits to the differential elastic-scattering cross-sections, if Vr_0^n is kept constant, where

(*) Present address: Xerox Corporation, Webster, N. Y. 14580, U.S.A.

(1) N. AUSTERN: *Direct Nuclear Reaction Theories* (New York, N. Y., 1970), p. 107.

LETTERE AL NUOVO CIMENTO VOL. 26, N. 5 29 Settembre 1979

A Singular Property of the Volume-Absorptive Optical Potential as Used in the Zero-Range DWBA Calculation of the (p, t_0) Angular Distribution.

Y. IWASAKI

Cyclotron Laboratory, Michigan State University - East Lansing, Michigan 48824, *U.S.A.*

(ricevuto il 23 Luglio 1979)

The distorted-wave Born approximation (DWBA) theory in its zero-range version has been used for more than a decade and is still used in almost all analyses of experimental data of the (p, t) and (t, p) reactions, which is a historical fact that testifies to the importance of the theory in practice. Most authors used in the DWBA calculation the triton optical potential that had been determined by the triton elastic-scattering cross-sections [1,2]. Because of the ambiguities inherent in the determination of the optical potential by the elastic-scattering cross-sections [3], the radius parameter r_{0t} of the real central well had been *fixed* at 1.16 fm [2] or 1.24 fm [1,2] for all nuclei, and the volume-type imaginary well had been arbitrarily *chosen* before the surface-derivative-type imaginary well [1,2]. The present note points out that the conventional use of such a triton optical potential for the (p, t) reaction is based on no physical grounds. It is demonstrated that the volume-absorptive optical potential has a singular property when it is used in the zero-range DWBA calculation of the (p, t_0) angular distribution, in contrast to the surface-absorptive optical potential. The statements in the following are based upon results of extensive computational experiments using the zero-range DWBA code DWUCK 72 [4].

Figure 1 illustrates how the calculated (p, t_0) angular distribution changes with a variation of the well depth V_t and the radius parameter r_{0t} of the real central well of the triton optical potential keeping $V_t r_{0t}^2$ constant. The triton optical potential is of the conventional volume-absorptive type without a spin-orbit interaction [1,2]. It is seen that the well-known Vr_0^n ($n \simeq 2$) ambiguity [3] does not exist in the zero-range DWBA calculation of the (p, t_0) angular distribution. A comparison of fig. 1 with fig. 2 reveals further that the change in the angular distribution shape in fig. 1 is brought about dominantly by the change in r_{0t}, the change in V_t having a very small effect. Namely, the effect of a change in r_{0t} is not compensated at all by the effect of a change in V_t,

---

[1] J. C. HAFELE, E. R. FLYNN and A. G. BLAIR: *Phys. Rev.*, **155**, 1238 (1967).
[2] E. R. FLYNN, D. D. ARMSTRONG, J. G. BEERY and A. G. BLAIR: *Phys. Rev.*, **182**, 1113 (1969).
[3] N. AUSTERN: *Direct Nuclear Reaction Theories* (New York, N. Y., 1970), p. 107.
[4] P. D. KUNZ: University of Colorado (unpublished).

review article

Nuclear vibrations

G. F. Bertsch
Michigan State University, East Lansing, Michigan 48824

Three types of nuclear vibrations have been observed in which a large fraction of the nucleons participate. There is a satisfactory explanation for the vibrational frequencies but not for the damping rates.

NUCLEI, like more familiar mechanical systems, can undergo simple vibratory motions. One mode of motion, in which protons move together in one direction while the neutrons simultaneously move in the opposite direction, has been known for 30 years. In the past decade, several new vibrational modes have been discovered. Our theoretical understanding of the nuclear motion has also considerably advanced. Although the most refined descriptions of the motion require a quantum many-body theory, the main features of the vibrations can be understood using classical physics. The motion of an extended body is described by a field of vectors which give the velocity of the medium at each point. Figure 1 shows the velocity fields for three types of vibration: monopole, dipole and quadrupole. These three modes are exhibited by nuclei as so-called 'giant vibrations', in which a large fraction of the nucleons participate in the motion. In both the monopole and quadrupole modes, all the nucleons move coherently in a direction which depends on their position in the nucleus. In the dipole motion, as mentioned above, protons and neutrons move in opposite directions.

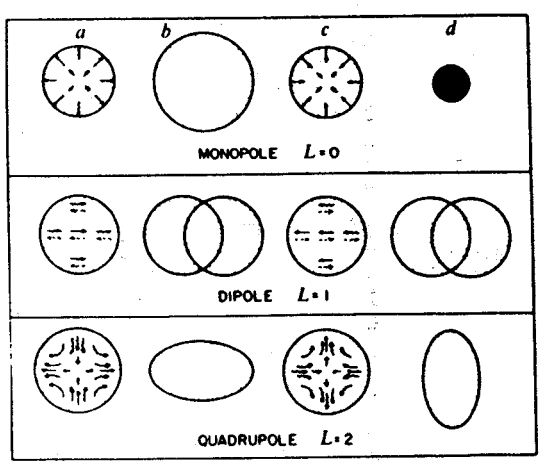

Fig. 1 The cycle of oscillation for simple vibrations. The velocity field at the moment when the nucleus passes through the equilibrium shape is shown in *a* and *c*. The shape at maximum distortion is shown in *b* and *d*. For the dipole, the neutrons and protons move in opposite directions. For other modes, the neutrons move with protons.

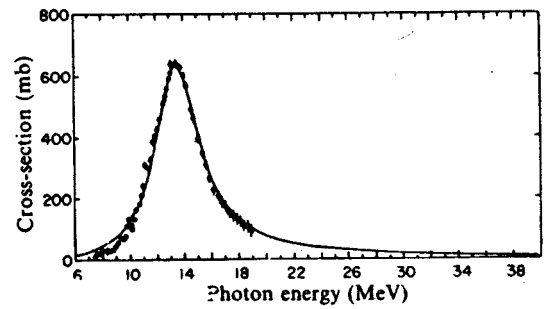

Fig. 2 The giant dipole resonance in ^{208}Pb, as observed by the photon reaction cross section (ref. 3, Fig. 32). The points are the experimental data, and the curve is the lorentzian function.

Dipole vibration

The first nuclear vibration to be observed, the giant dipole, was found in measurements of photon absorption. The reaction cross-section is enhanced by resonance when the photon frequency matches the vibrational frequency. The first indications of the giant dipole resonance were obtained before photon beams with a broad energy range were available. Bothe and Gentner in 1937 had a source of 14 MeV photons and they measured the radioactivity produced in a variety of targets[1]. The cross-sections varied considerably from target to target, indicating that there was a resonant absorption in some of the targets. By the mid-1940s, electron accelerators became available which produced bremsstrahlung photon beams of sufficient energy to observe the resonance. The improved data[2] showed that the absorption was concentrated in a resonance, the frequency of which varied systematically with the size of the nucleus.

One problem with these measurements is that the bremsstrahlung beam is broadly distributed in energy, so that the measurement for a particular energy required careful subtraction techniques. Currently, these experiments are done with photons that are produced by annihilation of positron, and are therefore monoenergetic. An example of the data now available[3] with this improved technique is shown in Fig. 2. The points are experimental data, and the curve is the lorentzian distribution,

$$\sigma(E)=\frac{\sigma_m}{1+[(E^2-E_m^2)^2/E^2\Gamma^2]}$$

were ≤5 s, given the sensitivity (~0.02 dB) and instrumental time constant (~0.1 s) that can be achieved with riometers. Ionospheric time constants of this order may apply in the *D* region during absorption events associated with some magnetic storms and substorms.

The research at the University of Maryland was supported by NSF grants DPP74-01704, DPP76-82041 and ATM77-22937. Additional support for balloon operations in Canada was provided by the Office of Naval Research (contract N00014-67-A-0239-0033). Bell Laboratories acknowledge the NSF for logistics support for the Siple measurements. We thank Dr H. Chivers for cooperation in the riometer data acquisition.

Received 4 September; accepted 13 November 1979.

1. Chivers, H. J. A. & Maagoe, S. *IEEE Trans. on Antennas and Propagat.* **513**, July (1972).
2. Lanzerotti, L. J., Maclennan, C. G. & Evans, C. *J. geophys. Res.* **83**, 2525 (1978).
3. Lanzerotti, L. J., Hasegawa, A. & Tartaglia, N. A. *J. geophys. Res.* **77**, 6731 (1972).
4. Leavitt, M. K., Carpenter, D. L., Seely, N. T., Padden, R. R. & Doolittle, J. H. *J. geophys. Res.* **83**, 1601 (1978).
5. Fukunishi, H. & Lanzerotti, L. J. *J. geophys. Res.* **79**, 4632 (1974).
6. Rosenberg, T. J., Foster, J. C., Matthews, D. L., Sheldon, W. R. & Benbrook, J. R. *J. geophys. Res.* **82**, 177 (1977).
7. Bering, E. A. *et al. J. geophys. Res.* **84**, (in press).
8. Reid, J. S. & Phillips, J. *Planet Space Sci.* **19**, 959 (1971).
9. Roldugin, V. K. *Geomagn. Aeron.* (English translation) **7**, 454 (1967).
10. Siren, J. C., Rosenberg, T. J., Detrick, D. & Lanzerotti, L. J. *J. geophys. Res.* (submitted).

Charge dependence of pion production in heavy ion collisions

G. Bertsch

Department of Physics and Cyclotron Laboratory,
Michigan State University, East Lansing, Michigan 48824

Benenson *et al.*[1] measured the pion production cross-section in nuclear heavy ion collisions in the energy range 100–400 MeV per nucleon with the aim of determining whether collective effects associated with the larger number of nucleons were present in the pion field. An instability in the pion field, such as the putative pion condensation phase transition[2], would give rise to an enhanced number of physical pions. The expected production cross-section, in the absence of collective effects, is found from two simple models. One of these is a statistical model, in which the number of pions is calculated from a statistical equilibrium. At the other extreme, the nucleons in the target and projectile are assumed to be free and independent, except for their Fermi momentum, and create pions by two-body collisions. The experimental cross-section at the lowest energy was found to be larger than either model by at least an order of magnitude[3], suggesting that collective effects are indeed present. Interestingly, the cross-section had unexpectedly strong dependence on the charge of the pion produced. At the highest energy studied, 400 MeV per nucleon, many more π^- than π^+ were produced in the forward direction. At the lowest energy studied, 100 MeV per nucleon, the relative yields are reversed, with more π^+ produced. The experimental ratios of π^- to π^+,

$$R_{-/+}=\frac{\mathrm{d}\sigma_{\pi^-}}{\mathrm{d}^3p}\Big/\frac{\mathrm{d}\sigma_{\pi^+}}{\mathrm{d}^3p}$$

are quoted in Table 1. Benenson *et al.*[1] explain the π^- enhancement in terms of the Coulomb distortions of the pion wavefunctions. Here I include in the same framework an explanation of the low energy result.

My starting point for the pion production rate is the formula

$$W=2\pi\sum_f\langle i|H_{\pi N}|f\rangle^2\rho_f$$

Table 1 Experimental ratios of π^- to π^+

E_{proj} (MeV per nucleon)	Pion kinetic energy (MeV)	$y_\pi - y_{proj}$*	$R_{-/+}$
~100	34	0.23	0.7
	54	0.40	0.6
	76	0.54	0.5
400	34	−0.20	3.0
	54	−0.04	10.0
	76	0.11	2.5
	123	0.36	1.4
	155	0.49	1.2

* Rapidity, the Lorentz-additive measure of velocity, is defined as $y=\frac{1}{2}\ln(E+pc)/(E-pc)$.

where ρ_f is the density of final states and $H_{\pi N}$ is the pion creation part of the nuclear hamiltonian. The ρ_f is a product of density of pionic states ρ_f^π, and density of nucleonic states ρ_f^N. Normalising the pion wavefunction to plane waves at infinity, the pionic density of states is the usual $\rho_f^\pi=\frac{\mathrm{d}^3p}{(2\pi)^3}$. The transition matrix element $\langle i|H_{\pi N}|f\rangle^2$ will be proportional to the probability of these normalised wavefunctions in the collision region, $|\phi_{\pi^*}|^2$. Benenson *et al.*[1] compute the charge dependence as

$$R_{-/+}\approx\frac{|\phi_{\pi^-}(R)|^2}{|\phi_{\pi^-}(R)|^2}$$

where ϕ_{π^*} contains the Coulomb distortion of the projectile. Thereby the large effect seen for pion velocities close to the beam velocity is qualitatively explained. The effect of the nuclear density of states will now be included. To describe ρ_f^N, it is assumed that there is a thermal equilibrium among nucleons. The final state density then depends on pion energy and charge according to

$$\rho_f^N\sim\exp\left[-(E_{\pi^*}\mp(\mu_p-\mu_n))/kT\right] \quad (1)$$

Here kT is the temperature of the nucleons, and μ_p and μ_n are the chemical potentials of the protons and neutrons. In view of the relatively small number of nucleons involved in the collision, and the fact that the pions are most likely to be created at the initial stages of the collision, before any sort of equilibrium is established, the statistical assumption may be questioned. However, it is a fact that energy spectra tend to be exponential, with a coefficient close to the 'temperature' calculated as below[4]. Thus we at least find phenomenological justification for equation (1).

$R_{-/+}$ is now compared at the two energies, for the same velocity of the pion with respect to the projectile. The Coulomb distortion effects should be nearly the same, so the ratio of $R_{-/+}$ would be given by

$$R_{-/+}/R'_{-/+}\approx\exp\left[2(\mu_p-\mu_n)\left(\frac{1}{kT'}-\frac{1}{kT}\right)\right]$$

In the system studied experimentally, ^{20}Ne + NaF, the chemical potentials differ mainly because of the Coulomb field. Assuming that the pion production takes place in an overlap region between the colliding nuclei, the difference between chemical potentials may be estimated as

$$\mu_p-\mu_n=\frac{Ze^2}{R}\approx\frac{20(1.44)}{3.3}\,\mathrm{MeV}\approx 8.7\,\mathrm{MeV}$$

To estimate the temperature at 100 MeV per nucleon projectile energy, note that the energy available in the centre of mass, per nucleon, is ~25 MeV. With Boltzmann statistics, this implies a temperature of $\frac{2}{3}(25)=16.7$ MeV. A more detailed calculation taking into account such things as quantum statistics and binding energy effects yields a temperature of 13.5 MeV. Similar considerations for 400 MeV per nucleon yield a temperature of

0028-0836/80/030280—02$01.00

NUCLEAR INSTRUMENTS AND METHODS 169 (1980) 327-336; © NORTH-HOLLAND PUBLISHING CO.

EFFECTS OF SPIRAL ELECTRIC GAPS IN SUPERCONDUCTING CYCLOTRONS*

M. M. GORDON

Cyclotron Laboratory, Michigan State University, East Lansing, Michigan 48824, U.S.A.

Received 18 September 1979

The $K = 500$ MeV superconducting cyclotron being built here has an RF system containing three dees with spiral electric gaps. These gaps produce a significant force component transverse to the ion orbits. An analysis is presented which shows nevertheless that the effect of such gaps does not alter the relevant orbit period, in accordance with an unpublished theorem due to McMillan. The structure of the "Spiral Gap" orbit program is then described. This program calculates ion orbits in a given magnetic field and provides a systematic treatment of the transverse as well as the longitudinal electric force resulting from spiral electric gaps. Sample results are presented which show that there is no significant difference in the phase-energy history of ion orbits accelerated with spiral or non-spiral electric gaps. A discussion of central ray orbits and accelerated equilibrium orbits is also presented together with analytical and computer results.

1. Introduction

The so-called "superconducting" cyclotron is a sectorfocused cyclotron having main magnet coils which are superconducting. The resultant high magnetic fields in these machines make them very well suited for use as heavy ion accelerators. Such cyclotrons are presently under construction at Chalk River[1]) and at this laboratory[2]).

The one being built here is designated as a "$K = 500$ MeV" superconducting cyclotron. This K value is derived from the widely used (non-relativistic) formula for the final energies of the ions produced by the cyclotron, namely,

$$E_f = K(q^2/A), \tag{1}$$

where q is the charge number of the ion, and A is its mass number. Present plans call for using this machine as an injector for a second superconducting cyclotron having $K = 800$ MeV.

Using rough numbers, the circular superconducting coils produce a central field of 40 kG at peak current. Since the iron sectors can contribute an additional field of only 20 kG in the magnetic "hills", these sectors must have a substantial amount of spiral in order to produce adequate vertical focusing[3]). Such machines are therefore characterized as having "low flutter and high spiral", and were first analyzed in detail by King and Walkinshaw[4]).

The cyclotron under construction here has three sectors with a rather small vertical gap between the magnet hills. The RF system consists of three dees located in the magnet valleys where adequate insulation space is available to withstand the high voltage required by the design. A schematic representation of these dees is shown in fig. 1. The phase relations and other properties of this three dee system are described in section 3 and elsewhere[5]).

As shown in fig. 1, the three dees have constant angular width with boundaries curved to conform to the spiral of the magnet sectors. The use of such

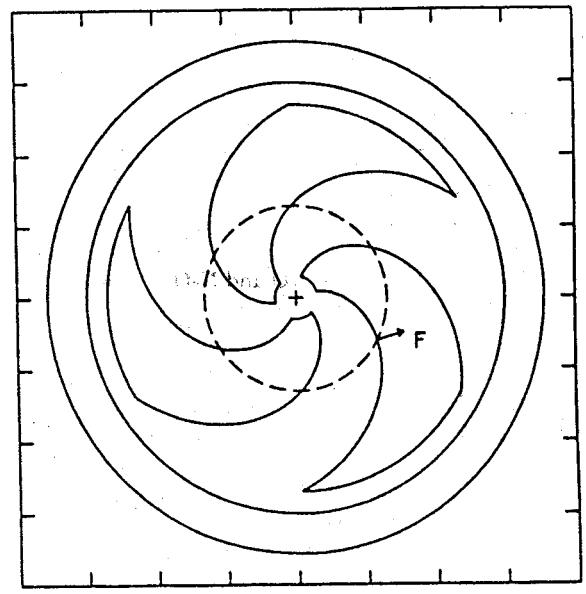

Fig. 1. Schematic representation of the three dees in the $K = 500$ MeV superconducting cyclotron. These dees are situated in the magnet valleys and are assumed to have a constant angular width, $D = 60°$, so that the six spiral electric gaps are all 60° apart. The electric force F is perpendicular to the gap line, and is shown here for one particular gap crossing at $r = 13$ inch, as indicated by the broken circle. The two outer circles at $r = 30$ and 36 inch represent the boundaries of the superconducting coil.

* This material is based upon work supported by the National Science Foundation under Grant No. PHY 78-22696.

APPLIED AND ENVIRONMENTAL MICROBIOLOGY, Jan. 1980, p. 105-108
0099-2240/80/01-0105/04$02.00/0 Vol. 39, No. 1

Inhibition by Sulfide of Nitric and Nitrous Oxide Reduction by Denitrifying *Pseudomonas fluorescens*†

JAN SØRENSEN,[1]‡ JAMES M. TIEDJE,[1]* AND RICHARD B. FIRESTONE[2]

Department of Crop and Soil Sciences,[1] Department of Microbiology and Public Health,[1] and Heavy Ion Laboratory,[2] Michigan State University, East Lansing, Michigan 48824

The influence of low redox potentials and H_2S on NO and N_2O reduction by resting cells of denitrifying *Pseudomonas fluorescens* was studied. Hydrogen sulfide and Ti(III) were added to achieve redox potentials near −200 mV. The control without reductant had a redox potential near +200 mV. Production of ^{13}NO, $[^{13}N]N_2O$, and $[^{13}N]N_2$ from $^{13}NO_3^-$ and $^{13}NO_2^-$ was followed. Total gas production was similar for all three treatments. The accumulation of ^{13}NO was most significant in the presence of sulfide. A parallel control with autoclaved cells indicated that the ^{13}NO production was largely biological. The sulfide inhibition was more dramatic at the level of N_2O reduction; $[^{13}N]N_2O$ became the major product instead of $[^{13}N]N_2$, the dominant product when either no reductant or Ti(III) was present. The results indicate that the specific action of sulfide rather than the low redox potential caused a partial inhibition of NO reduction and a strong inhibition of N_2O reduction in denitrifying cells.

In a search of environmental factors that influence the overall activity and the differential release of gas products during denitrification, reference is most often given to parameters such as O_2, available carbon, pH, and temperature (2). Much less attention has been paid to the parameters characteristic of the reduced environment, e.g., iron and sulfur compounds. In some environments, in particular marine sediments, denitrification takes place in close proximity to zones of active transformation of iron and sulfur.

In an earlier study in coastal marine sediments, significant accumulation of the denitrification intermediates, NO and N_2O, was noted in the redox transition zone near the sulfide-rich deeper layers; it was suggested that these accumulations were caused by either the low redox potential or the presence of sulfide in this zone (5).

The present study was undertaken to establish whether a low redox potential or the presence of sulfide caused accumulation of NO, N_2O, or both. It was found that sulfide and not a low redox potential caused an increase in proportion of N_2O and NO at the expense of N_2 in denitrifying *Pseudomonas fluorescens*.

MATERIALS AND METHODS

The denitrifying bacterium used was *P. fluorescens* (strain 72), isolated from poorly drained Minnesota maize soil by Gamble et al. (3). The organism was grown anaerobically in tryptic soy or nutrient broth (Difco) with nitrate (3.5 mM KNO_3) or nitrite (5 mM KNO_2) as the electron acceptor. The cells were harvested at early stationary phase by centrifugation at 5°C. Cells were washed three times in 0.02 M phosphate buffer (pH 7.0) and suspended to an optical density of 0.2 to 0.5 at 660 nm.

It was anticipated that gas samples taken in syringes might be subject to O_2 contamination during the short wait before injection into the ^{13}N detection system. This risk was minimized by the admission of excess, unlabeled NO into the syringes, a step which also improved the elution of ^{13}NO from the chromatographic column. The possible lack of a quantitative recovery of ^{13}NO should not exclude a relative comparison of ^{13}NO production between the individual treatments, since all samples of a given incubation time were treated in a similar manner.

Any loss of free sulfide was negligible during the experimental time of 5 min, since a significant decrease of H_2S in similar incubations could not be detected by iodine titration until several hours had elapsed (Sørensen, unpublished data). Both reducing agents provided a measured redox potential (Eh value) near −200 mV. The reaction mixtures without reducing agent gave a positive but variable Eh value between +100 and +300 mV. It was likely that the short exposure to air during the redox assay gave values that overestimated the actual Eh during the incubation. The possible error was less important in the present context, however, where comparisons were made to the strongly reduced series with Ti(III) or H_2S and Eh values near −200 mV.

Five milliliters of the cell suspension was transferred to 25-ml serum vials with 1 ml of a 1% glucose solution. The vials were capped, made anaerobic by repeated evacuation, and purged with helium gas. This proce-

† Journal Article no. 5059 of the Michigan Agricultural Experiment Station.

‡ Present address: Institute of Ecology and Genetics, University of Aarhus, DK-8000 Aarhus, Denmark.

Reprinted from the *Soil Science Society of America Journal*
Volume 43, no. 6, November-December 1979
677 South Segoe Rd., Madison, WI 53711 USA

The Influence of Nitrate, Nitrite, and Oxygen on the Composition of the Gaseous Products of Denitrification in Soil[1]

M. K. FIRESTONE, M. S. SMITH, R. B. FIRESTONE, AND J. M. TIEDJE[2]

ABSTRACT

[^{13}N]-N_2O produced by denitrification of $^{13}NO_3^-$ in soil slurries readily exchanged with nonlabeled pools of added N_2O. This supports the role of N_2O as a free, obligate intermediate of denitrification in soils. The observation that N_2O diffuses freely from the site of active denitrification in soils means that any factor which produces a change in the relative rate of N_2O reduction compared to the rate of N_2O production can alter the proportion of N_2O and N_2 resulting. Increased concentration of NO_3^- and NO_2^- resulted in increased production of N_2O relative to N_2 as the product of denitrification. The influence of NO_2^- was much stronger than that of NO_3^-, with low concentrations of NO_2^- causing N_2O to become a significant product of denitrification. This suggests that NO_2^-, not NO_3^-, may be the influential species. Additions of small quantities of O_2 (0.02 atm) caused a large decrease in denitrification activity and resulted in a significant increase in the N_2O/N_2 ratio.

Additional Index Words: nitrous oxide, nitrogen gas, soil nitrogen metabolism, ^{15}N.

Firestone, M. K., M. S. Smith, R. B. Firestone, and J. M. Tiedje. 1979. The influence of nitrate, nitrite, and oxygen on the composition of the gaseous products of denitrification in soil. Soil Sci. Soc. Am. J. 43:1140-1144.

THE SUGGESTION that nitrous oxide is involved in destruction of the Earth's ozone layer has stimulated much interest in the production of N_2O by denitrification. The role played by soil in this process has recently been reviewed by Bremner (3). It has been proposed that soils may act both as a source and a sink for atmospheric N_2O (1, 3, 4), although recent work has indicated that under most conditions, field soils are a source of N_2O (11).

It is now widely accepted that N_2O and N_2 are the end products of biological denitrification in soils. But the environmental parameters which influence the relative proportion of N_2O and N_2 produced during denitrification are not well understood. The emission of N_2O by soils is influenced by factors which control the biological production and reduction of N_2O as well as by the physical characteristics of the soil which dictate the ease with which N_2O escapes the soil and further biological reduction.

We have employed ^{15}N-labeled NO_3^- and NO_2^- to investigate the influence of NO_3^-, and NO_2^-, and O_2 concentrations on the biological production of N_2O relative to N_2. Using short-term incubations we have been able to examine the influence of each parameter on the denitrification rate and ratio of products. To focus on the biological process, we have worked with well mixed soil slurries, thus minimizing the influence of diffusion through the natural soil matrix on the results.

MATERIALS AND METHODS

Preparation of Soils

The soils used in this study are described in Table 1. These soils were collected, passed through a 5-mm sieve, and stored without drying in sealed plastic bags at 2°C until used.

For experiments on the effect of the concentration of NO_3^- and NO_2^-, 75 g fresh weight of soil and 50 ml of H_2O were added to 125-ml Erlenmeyer flasks which were sealed with rub-

[1] Contribution from the Dept. of Crop and Soil Sciences, Dept. of Microbiology and Public Health, and the Heavy Ion Laboratory, Michigan State Univ., E. Lansing, MI 48824. Journal Article no. 8808 of the Michigan Agric. Exp. Stn. This work was supported by NSF Grants DEB-77-19273 and PHY-78-01684 and USDA Regional Research Project NE-39. Received 4 Dec. 1978. Approved 11 July 1979.

[2] Former Graduate Students, Assistant Professor of Chemistry, and Professor of Soil Microbiology, respectively. Current addresses are M.K.F., Dept. of Soils and Plant Nutrition, Univ. of Calif., Berkeley, M.S.S., Dept. of Agronomy, Univ. of Kentucky, and R.B.F., Lawrence Berkeley Laboratory, Univ. of Calif., Berkeley.

Reprinted from the *Soil Science Society of America Journal*
Volume 43, no. 5, September–October 1979
677 South Segoe Rd., Madison, WI 53711 USA

Methods for the Production and Use of Nitrogen-13 In Studies of Denitrification[1]

J. M. TIEDJE, R. B. FIRESTONE, M. K. FIRESTONE, M. R. BETLACH, M. S. SMITH, AND W. H. CASKEY[2]

ABSTRACT

Methods were developed for use of the radioactive isotope of nitrogen, ^{13}N, for short-term studies of denitrification. ^{13}N was generated by irradiation of water with 12 to 15 MeV proton beams from a sector-focused cyclotron. Under typical operating conditions of 0.7 to 3 μA beam currents for 10 min, the ^{13}N ionic species produced were $^{13}NO_3^-$, 75–90%; $^{13}NO_2^-$, 5–10% and $^{13}NH_4^+$, 0.5–25%. Traces of [^{13}N] N_2O and [^{13}N] N_2 were also produced. The measured yield varied from 2 to 16 mCi/10 min irradiation depending on beam current. Vacuum evaporation at high pH was used to obtain $^{13}NO_3^- + {}^{13}NO_2^-$ at > 99.8% purity, and high performance liquid chromatography (HPLC) was used to obtain $^{13}NO_3^-$ or $^{13}NO_2^-$ at > 99% purity. The HPLC system used a Partisil SAX anion exchange column eluted with phosphate buffer at pH 3.0 and was coupled to a coincidence NaI(Tl) detector for counting ^{13}N species in the effluent. Separation of NH_4^+, NO_3^-, and NO_2^- was achieved within 5 min. This system was used to monitor purity of ^{13}N substrates and for studies of dissimilatory nitrate reduction to ammonia. A gas chromatograph-proportional counter detector system was developed to separate and measure [^{13}N] N_2, [^{13}N] N_2O and ^{13}NO. Separation was by Poropak Q and Molecular Sieve 5A columns and was achieved in 5 min. Denitrification rates and products of soils and bacterial cultures incubated in sealed flasks were monitored with this system. Continuous rates of [^{13}N] N_2 and [^{13}N] N_2O production were monitored using a differential trapping, gas stripping system. Soil slurries amended with $^{13}NO_3^-$ or $^{13}NO_2^-$ were stripped of gases by continuously sparging with helium. N_2O was collected in a liquid nitrogen trap. Nitrogen gas passed through this trap but was retained in a Molecular Sieve trap immersed in liquid nitrogen. ^{13}N gases collected in each trap were continuously counted by NaI (Tl) detectors. Linear rates of gas production were typically observed from 15 min after addition of the ^{13}N substrate to termination of the experiment after 1 to 1.5 hours. ^{13}N has the advantage in denitrification studies of allowing direct measurement of N_2, very sensitive short-term rate measurements, and isotope exchange experiments at low substrate concentrations.

Additional Index Words: nitrous oxide, nitrogen gas, soil nitrogen, metabolism.

Tiedje, J. M., R. B. Firestone, M. K. Firestone, M. R. Betlach, M. S. Smith, and W. H. Caskey. 1979. Methods for the production and use of nitrogen-13 in studies of denitrification. Soil Sci. Soc. Am. J. 43:709–715.

RESEARCH on nitrogen metabolism and the nitrogen cycle has been hindered by the unavailability of a radioactive isotope of nitrogen. An alternative is the use of ^{15}N enriched or depleted nitrogen; however, sensitivity is often a problem since the detection limit is relatively high and always a function of the total nitrogen content of the sample analyzed. This limitation has been particularly severe to the study of denitrification since the major product, N_2, cannot usually be measured without altering the natural atmosphere of the sample being studied. Since O_2 is the principal regulator of denitrification, this is an important limitation. Use of a radioactive isotope of nitrogen allows direct measurement of N_2 in any atmosphere. ^{13}N is the longest lived radioactive isotope of nitrogen with a half-life of about 10 min, which allows an experimental time of 1-2 hours and is adequate for short-term studies of denitrification.

Besides direct detection of N_2, the high specific activity of ^{13}N, 1.88×10^{10} Ci/g-atm, provides extremely high sensitivity over the short-term. Assuming optimal operating conditions the minimum detectable amount of ^{13}N is less than 2000 atoms (3.3×10^{-21} moles). This compares to 1×10^{-12} moles for ^{14}C or 7×10^{-9} moles for ^{15}N (assuming 99 atom % excess). This greater sensitivity of ^{13}N over ^{15}N is often of importance in denitrification studies since the denitrification rate is dependent on nitrate concentration. The large additions of $^{15}NO_3^-$-N required (often > 50 ppm) for stable isotope experiments can cause an artificially high denitrification rate and will alter the ratio of N_2O/N_2 (4). In contrast concentrations of only 10^{-8} ppm or less of $^{13}NO_3^-$-N are needed to measure denitrification rates.

Little is known about transient events in denitrification, especially the response to changes in moisture and thus oxygen content of soils. ^{13}N because of its high sensitivity is well-suited to investigation of such short-term phenomena. Classical methods have generally required 0.5 to 1 day before the first discernable results could be obtained. ^{13}N allows measurement of denitrification rates in freshly collected samples before any significant change in enzyme concentration can occur. Also because of the high sensitivity, isotope exchange experiments can be performed at low substrate concentrations (4).

^{13}N has been used in the medical sciences (2, 15) and for studies of N_2 fixation (10, 22). Recently its application to studies of denitrification was demonstrated by Gersberg et al. (6). The utility of ^{13}N for denitrification studies is enhanced by the direct production of $^{13}NO_3^-$, which occurs when an H_2O target is used. This was first demonstrated by Lathrop et al. (9) and Gelbard et al. (5) in 1973 and has been successfully used in our studies.

In this paper we report on the procedures for production and purification of $^{13}NO_3^-$ and $^{13}NO_2^-$ and on rapid automated methods for measuring [^{13}N] N_2, [^{13}N] N_2O, ^{13}NO, $^{13}NH_4^+$, $^{13}NO_2^-$ and $^{13}NO_3^-$. These methods should also be useful for study of processes other than denitrification and for studies of transformations of other elements.

---

[1] Contribution from the Dep. of Crop & Soil Sciences, Dep. of Microbiology & Public Health, and the Heavy Ion Laboratory, Michigan State Univ., E. Lansing, MI 48824. Published as Journal Article no. 8928 of the Michigan Agric. Exp. Stn. This work was supported by NSF Grants DEB-77-19273 and PHY-78-01684 and USDA Regional Research Project NE-39. Received 5 Dec. 1978. Approved 5 Apr. 1979.

[2] Professor of Soil Microbiology, Assistant Professor of Chemistry and Heavy Ion Laboratory, and Graduate Students, respectively. Current addresses are: M. K. F., Dept. of Soils and Plant Nutrition, Univ. of Calif., Berkeley; M. S. S., Dept. of Agronomy, Univ. of Kentucky; and W. H. C., Inst. of Ecology, Univ. of Georgia.

Tome 41 N° 4 15 FÉVRIER 1980

LE JOURNAL DE PHYSIQUE - LETTRES

Classification
Physics Abstracts
21.10D — 25.70

Mass excess and excited states of ^{14}B and ^{18}N from the (^{14}C, ^{14}B) and (^{18}O, ^{18}N) reactions

F. Naulin, C. Détraz, M. Bernas, D. Guillemaud, E. Kashy (*), M. Langevin, F. Pougheon, P. Roussel and M. Roy-Stephan

Institut de Physique Nucléaire, B.P. n° 1, 91406 Orsay, France

(*Reçu le 21 décembre 1979, accepté le 3 janvier 1980*)

Résumé. — Les réactions (^{14}C, ^{14}B) et (^{18}O, ^{18}N) sur le noyau ^{14}C ont été utilisées pour mesurer l'excès de masse des noyaux ^{14}B et ^{18}N. Un état excité de ^{18}N est observé à 575 ± 25 keV.

Abstract. — The (^{14}C, ^{14}B) and (^{18}O, ^{18}N) reactions on a ^{14}C target have been utilized to determine the mass excess of the ^{14}B and ^{18}N nuclei. An excited state of ^{18}N is observed at 575 ± 25 keV.

1. **Introduction.** — Neutron rich odd-odd light nuclei with $T = 2$, such as ^{14}B and ^{18}N, are much less known than a number of neighbouring isotopes further away from the valley of β-stability.

Although this series of nuclei is only a single charge-exchange reaction away from stable isotopes, experimental information is scarce and sometimes contradictory. This is due to two reasons. The first one is that the charge-exchange reaction has to be of the (n, p) or (t, ^{3}He) kind with light particles, which carries obvious experimental difficulties. The second one lies with the somewhat high density of low-lying excited states of the residual odd-odd nucleus, which makes the characterization of the ground and individual excited states sometimes ambiguous.

A progress in this situation requires the use of heavy ion beams, as long as good particle identification is achieved and an effort is made towards the best possible energy resolution.

The qualities of the heavy-ion beams which result from the recent equipment of the Orsay MP tandem with a Laddertron charge system, together with recent improvements in the experimental apparatus have allowed the collection of low-background, good energy resolution data bearing on the mass excess and excited states of ^{14}B and ^{18}N, which are presented in this paper.

2. **Available information on ^{14}B and ^{18}N.** — The mass excess and the energies of the first excited states of ^{14}B have been measured once only, through the $^{14}C(^7Li, ^7Be)^{14}B$ reaction [1]. Another study of ^{14}B through a different nuclear reaction seems worthwhile. The situation for ^{18}N is more complicated. An early $^{18}O(t, ^3He)^{18}N$ experiment [2] observed a single broad peak in the proton energy spectrum, corresponding to a 13.274 ± 0.030 MeV mass excess for ^{18}N. An even earlier measurement [3] of the β end-point energy in the decay of ^{18}N had determined a 13.1 ± 0.4 MeV mass excess. Recently the (d, ^{2}He) reaction on ^{18}O was used [4] to further study the energy spectrum. Again a broad peak centred around the mass excess value of ref. [2] was observed. However the height of the background precluded any firm conclusion although there was indication that the broad peak might consist of at least 3 peaks seen as *shoulders*.

3. **Experimental method.** — Low statistics are unavoidable when one studies nuclei far from the valley of β-stability since their formation requires the use of exotic nuclear reactions. To turn the few observed events into a meaningful quantitative measurement supposes first an unambiguous identification of the ions detected and second an optimization of the peak-to-noise ratio in their energy measurement. This second requirement is pursued by obtaining the best possible energy resolution and drastically reducing the background. Hence three experimental factors are of

(*) On leave from Michigan State University, East Lansing, Michigan, U.S.A.